# Hydrogenation of Biodiesel Catalysed by Pyrazolyl Nickel(II) and Palladium(II) Complexes

Oluwasegun Emmanuel Olaoye,*[a] Olayinka Oyetunji,*[a] Banothile C. E. Makhubela,[b] Gopendra Kumar[a] and James Darkwa*[b,c]

[a]*Department of Chemistry, University of Botswana, Private Bag UB 00704, Gaborone, Botswana.*

[b]*Department of Chemical Sciences, University of Johannesburg, Kingsway Campus, Auckland Park, 2006, South Africa.*

[c]*Botswana Institute for Technology Research and Innovation, Machel Drive, Gaborone, Botswana.*

*Corresponding Authors: 201605304@ub.ac.bw; yoyetunji@gmail.com; jdarkwa@gmail.com

## Supplementary Information

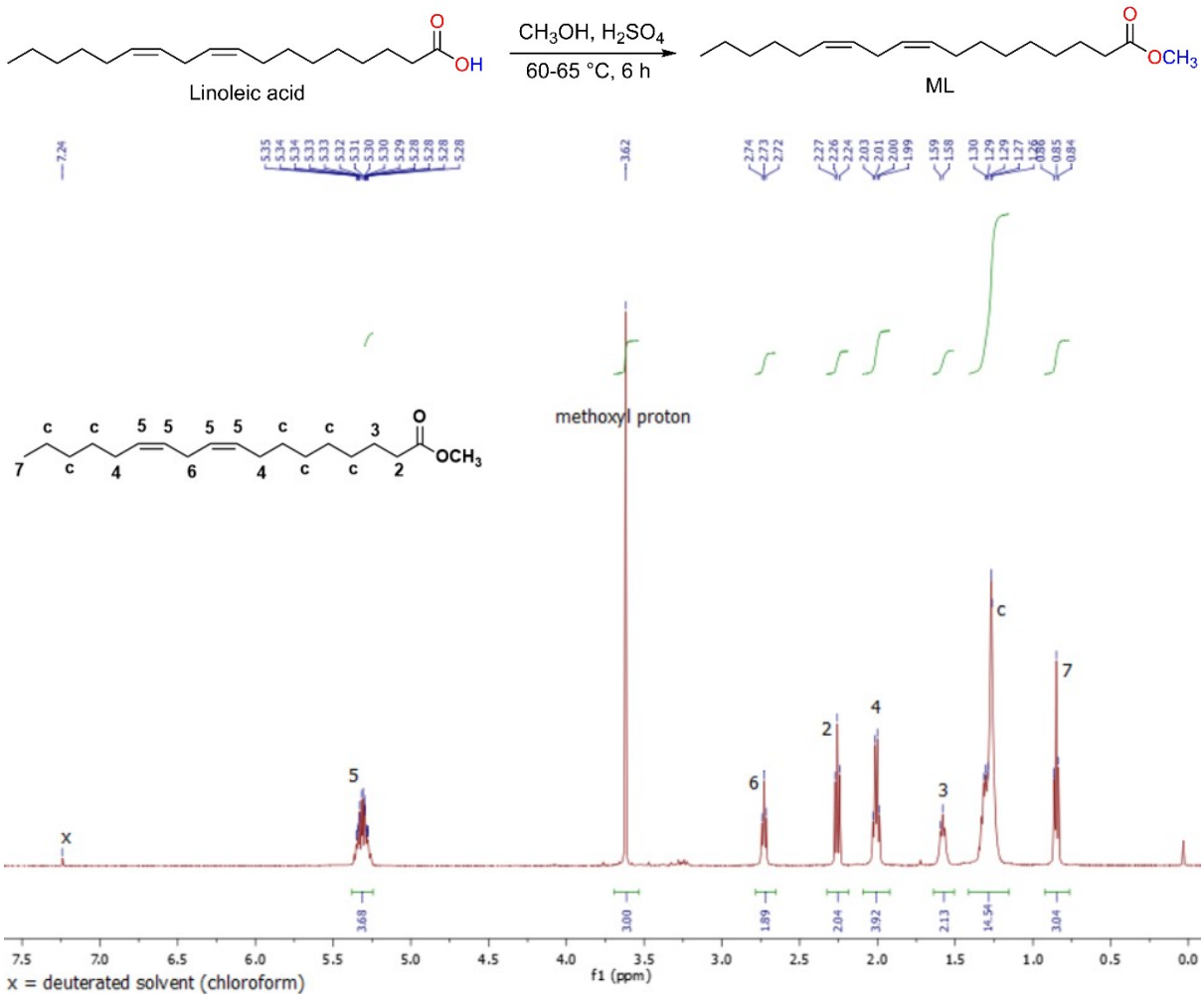


**Fig. S1** $^{1}$H NMR spectrum of the substrate (methyl linoleate) in $CDCl_3$ before carrying out the hydrogenation reaction with pyrazolyl nickel(II) and palladium(II) complexes.

The diagnostic peak at 3.62 ppm in the Fig. S1 corresponds to the methoxy protons (-$OCH_3$) of the substrate, methyl linoleate. The substrate's peaks around 2.01 ppm, 2.73 ppm, and 5.31 ppm are due to allylic, bis-allylic and olefinic protons, respectively. Sharp singlet signal at 1.26 ppm represents methylene protons of the carbon chain, whilst the triplet resonating at 0.85 ppm is due to the terminal methyl protons. The triplet around 2.27 ppm corresponds to the methylene protons that are adjacent to the carbonyl group (Fig. S1).

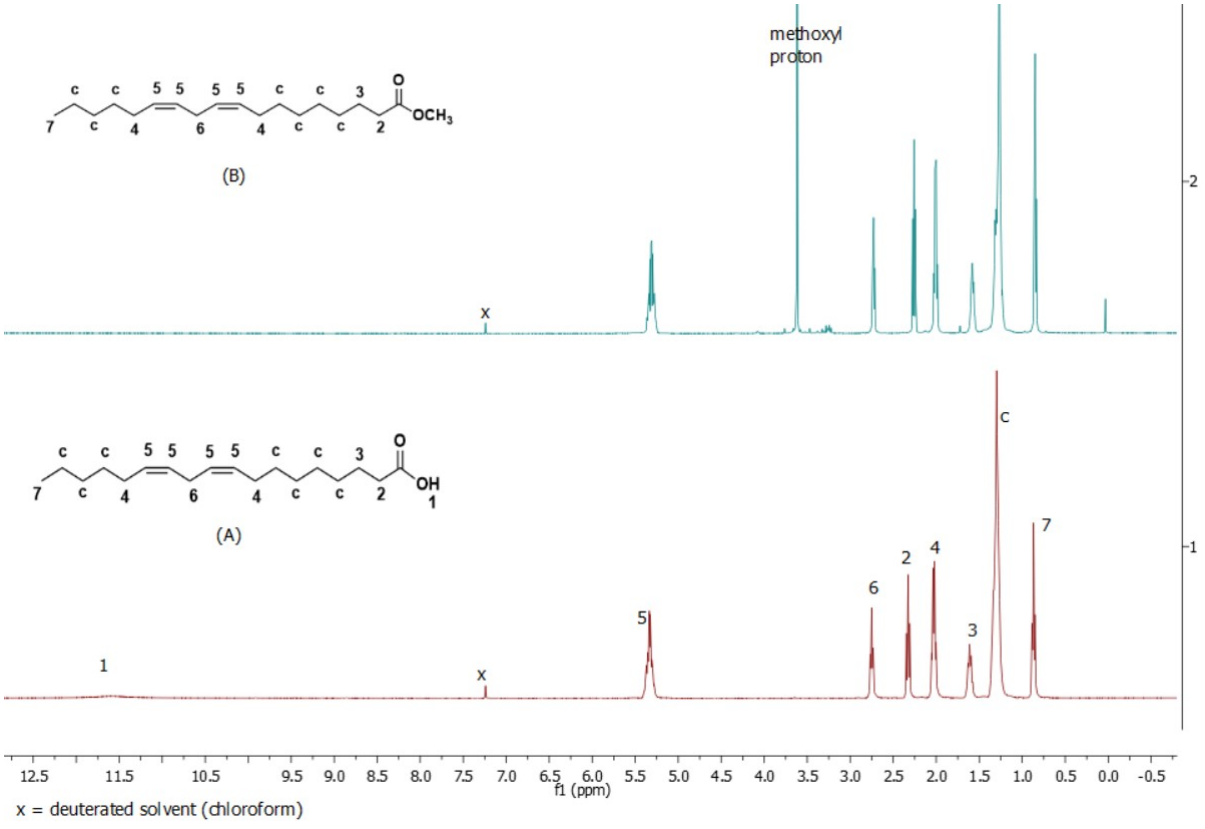


**Fig. S2** $^1$H NMR spectrum of methyl linoleate (ML) (**b**) produced from linoleic acid (**a**) in $CDCl_3$.

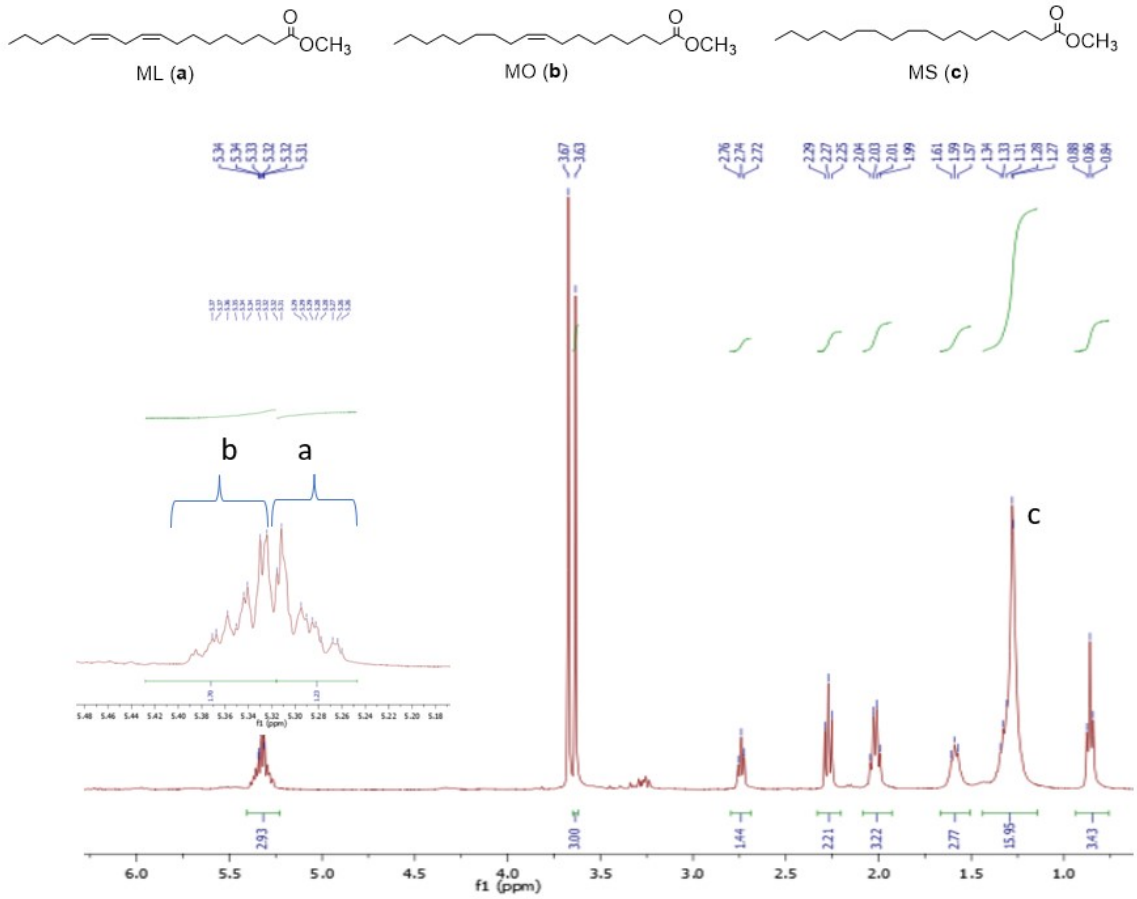


**Fig. S3** $^{1}$H NMR spectrum of products from the hydrogenation of methyl linoleate (ML) using complex **6** showing the distribution of the products of MO and MS. 2.5 μmol (0.83 mol%) of the catalyst; 0.3 mmol of methyl linoleate; 5 mL of methanol; 50 °C; 5 bar, 0.5 h.

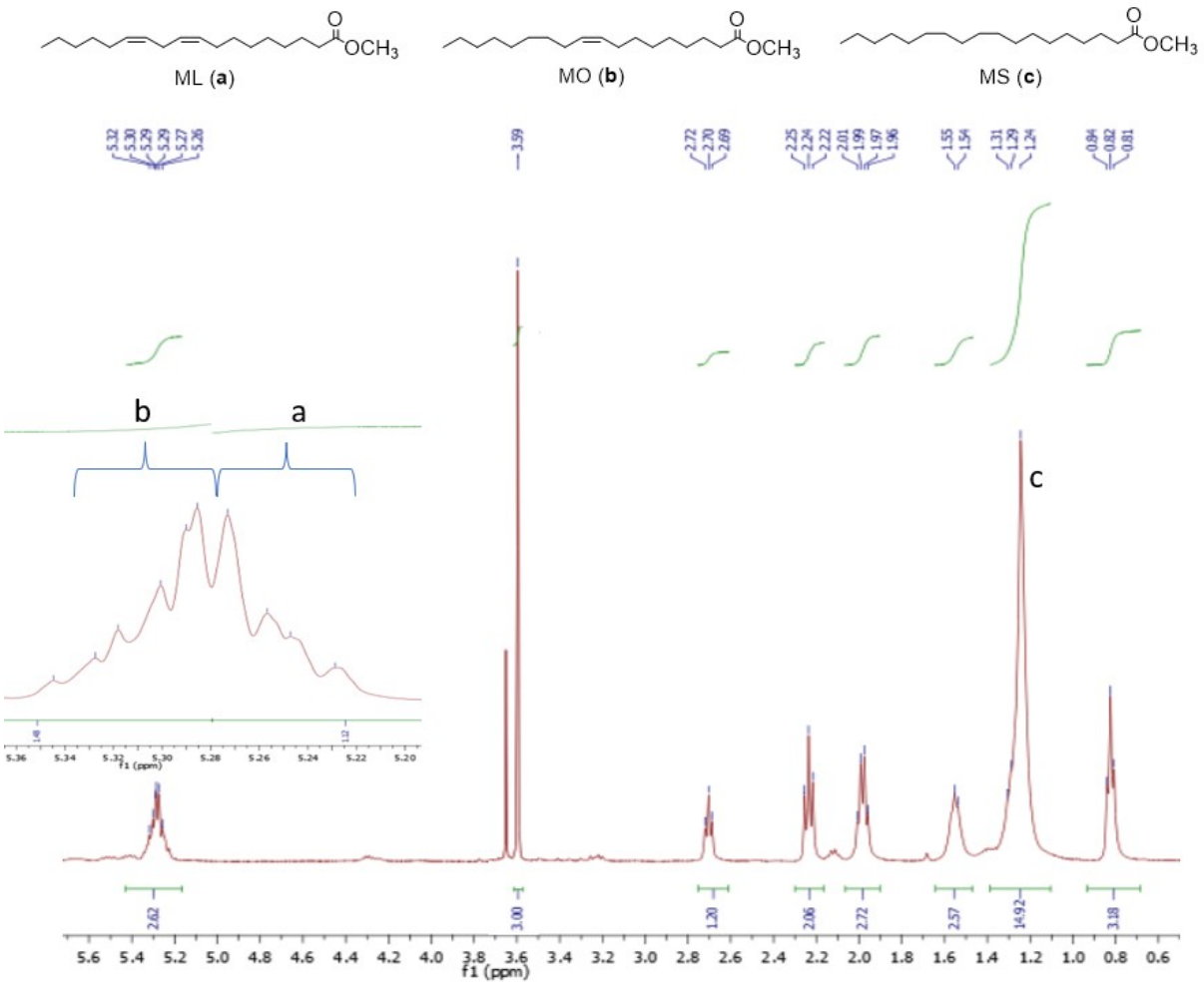


**Fig. SI-4** $^{1}$H NMR spectrum of products from the hydrogenation of methyl linoleate (ML) using complex **4** showing the distribution of the products of MO and MS. 29% conversion; 2.5 µmol (0.83 mol%) of the catalyst; 0.3 mmol of methyl linoleate; 5 mL of methanol; 50 °C; 5 bar, 0.5 h.

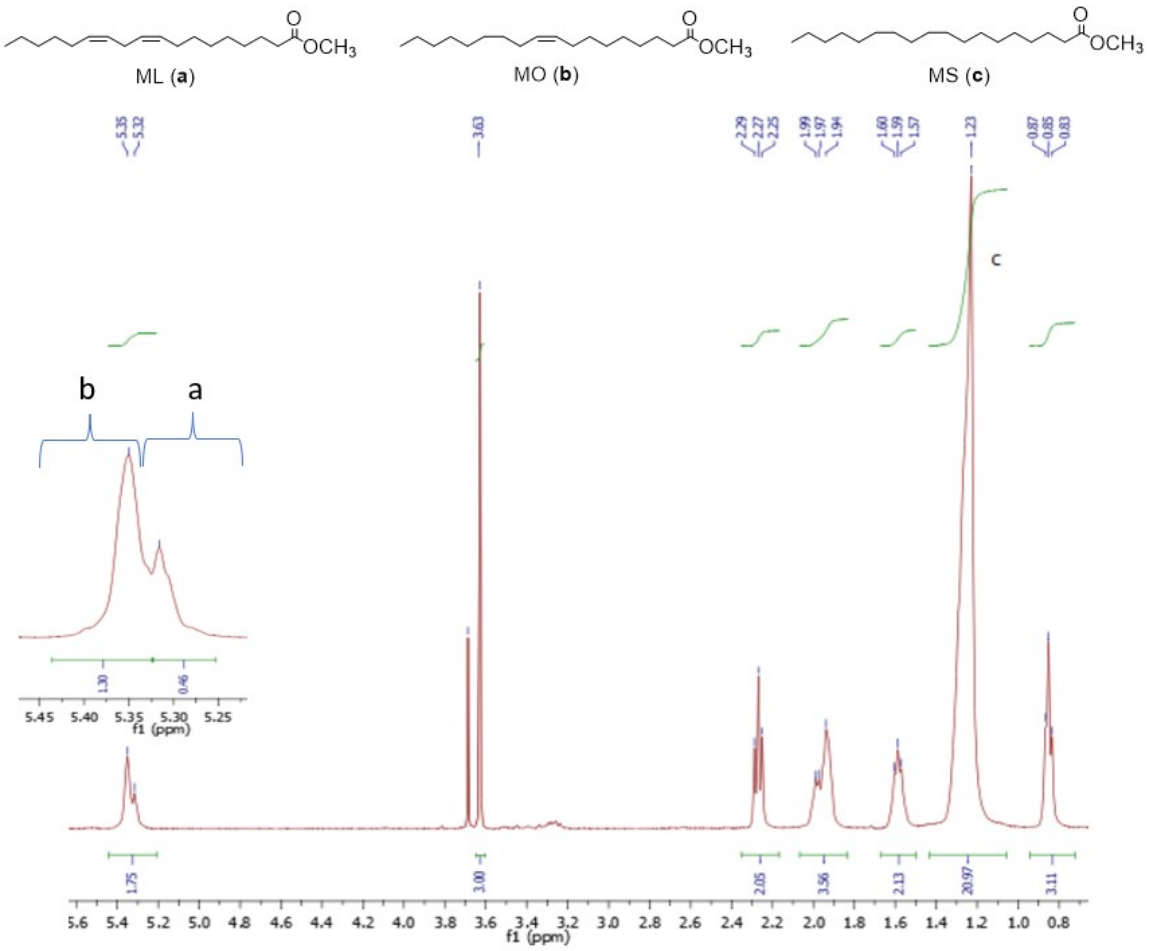


**Fig. S5** $^{1}$H NMR spectrum of products from the hydrogenation of methyl linoleate (ML) using complex **4** showing the distribution of the products of MO and MS. 52% conversion; 2.5 µmol (0.83 mol%) of the catalyst; 0.3 mmol of methyl linoleate; 5 mL of methanol; 50 °C; 5 bar, 1 h.

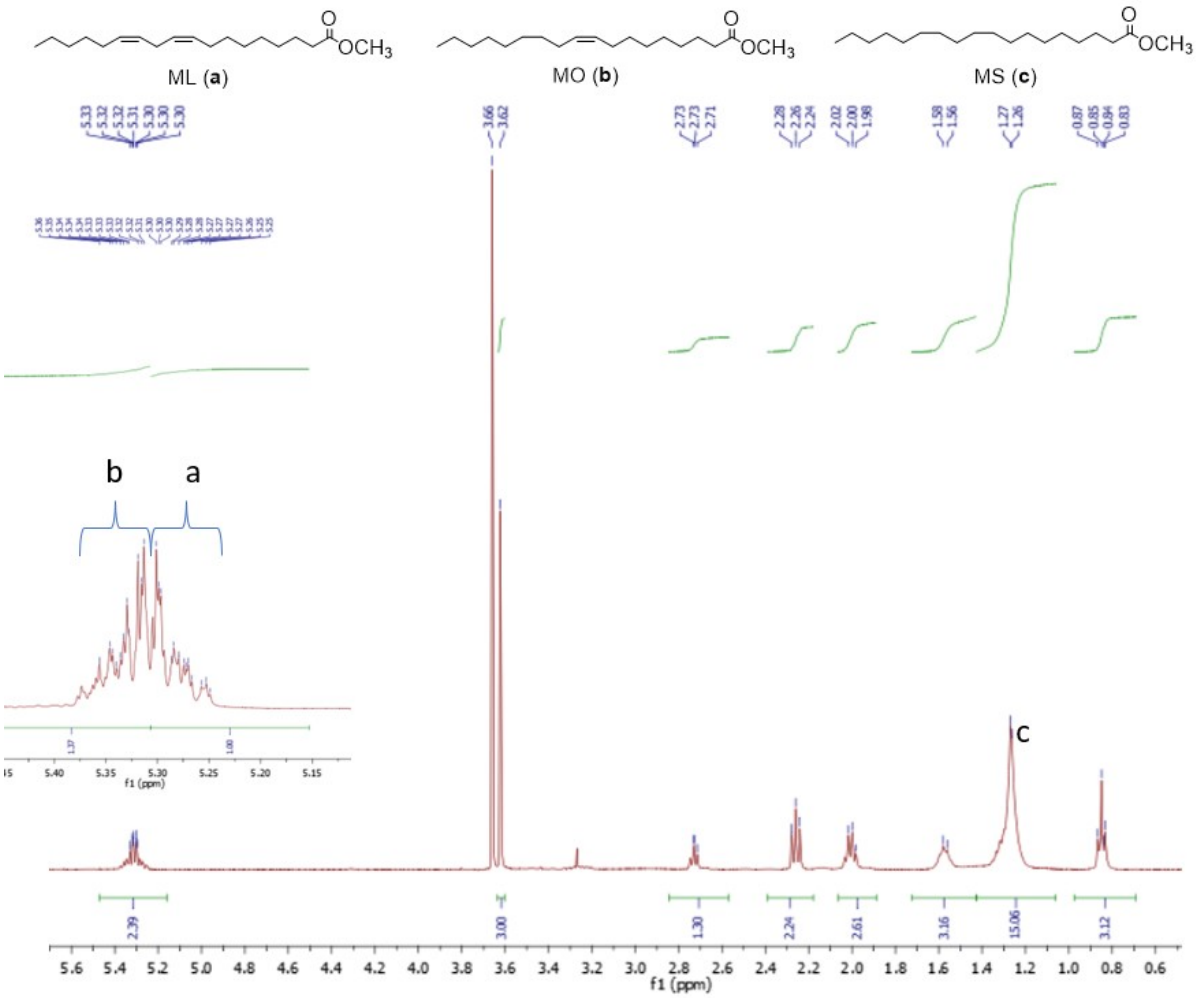


**Fig. S6** $^{1}$H NMR spectrum of products from the hydrogenation of methyl linoleate (ML) using complex **1** showing the distribution of the products of MO and MS. 35% conversion; 2.5 µmol (0.83 mol%) of the catalyst; 0.3 mmol of methyl linoleate; 5 mL of methanol; 50 °C; 5 bar, 0.5 h.

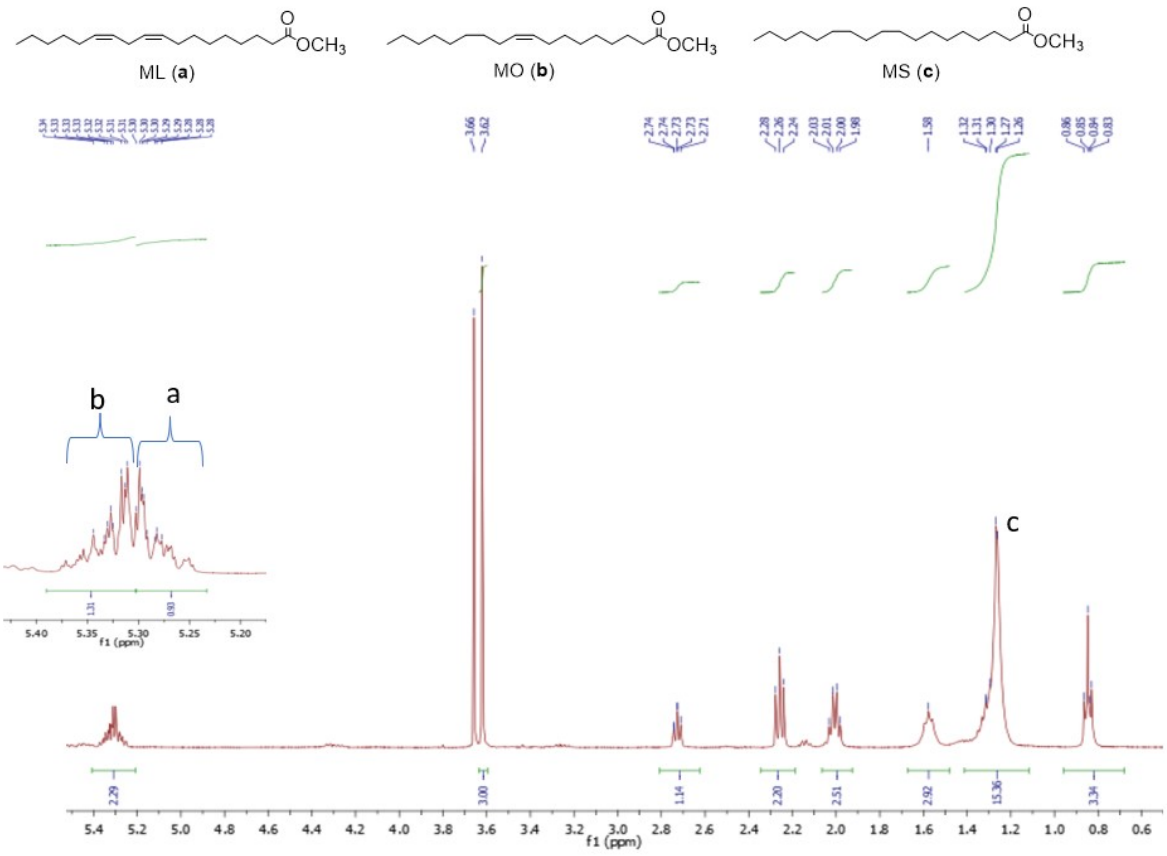


**Fig. S7** $^{1}$H NMR spectrum of products from the hydrogenation of methyl linoleate(ML) using complex **1** showing the distribution of the products of MO and MS. 38% conversion; 2.5 µmol (0.83 mol%) of the catalyst; 0.3 mmol of methyl linoleate; 5 mL of methanol; 50 °C; 5 bar, 1 h.

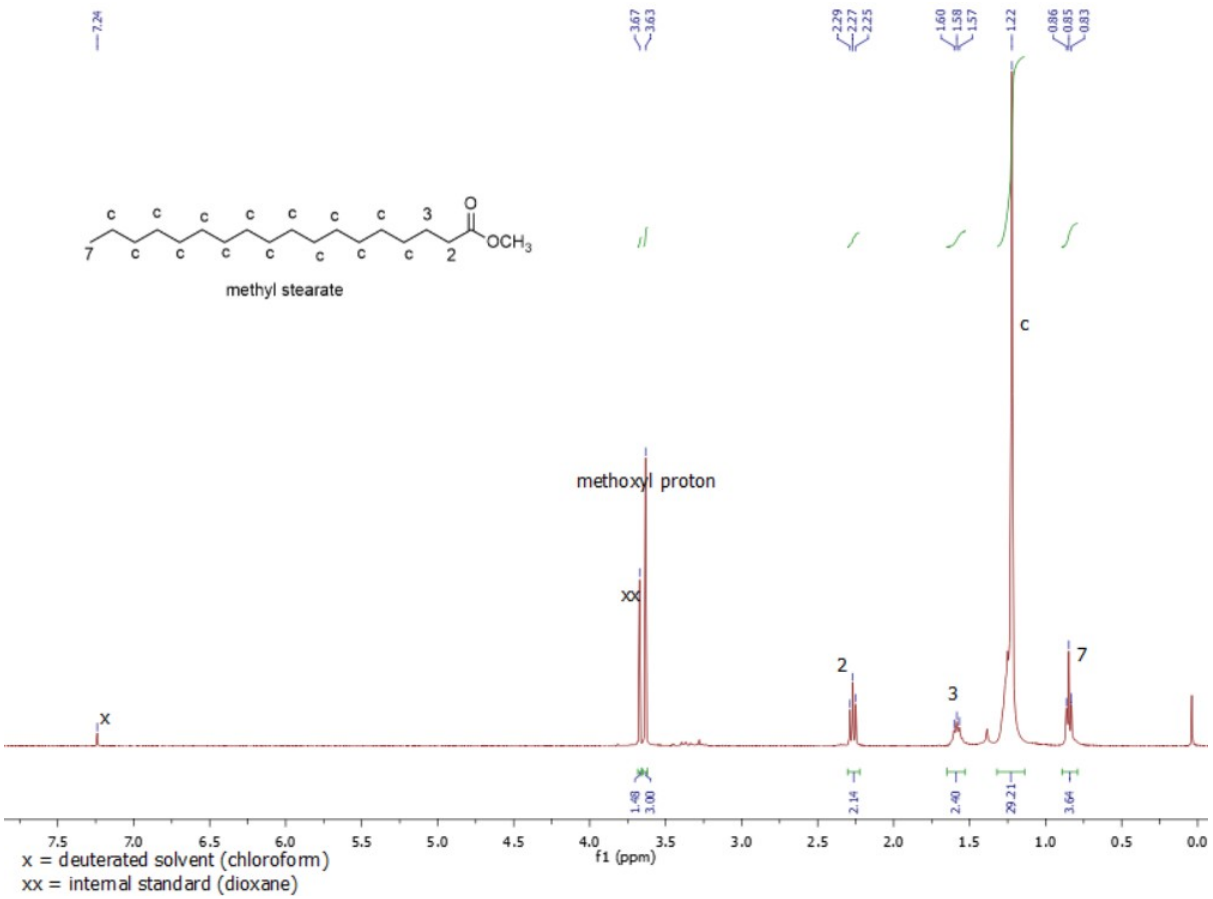


**Fig. S8** $^{1}$H NMR spectrum of methyl stearate (0.3 mmol) produced when all the C=C double bonds in methyl linoleate (ML) have been completely hydrogenated by complex **5** (0.83 mol%) to produce methyl stearate (MS). 100% conversions; 100% selectivity towards MS; 1 h; 5 mL of methanol; 50 °C; 5 bar.

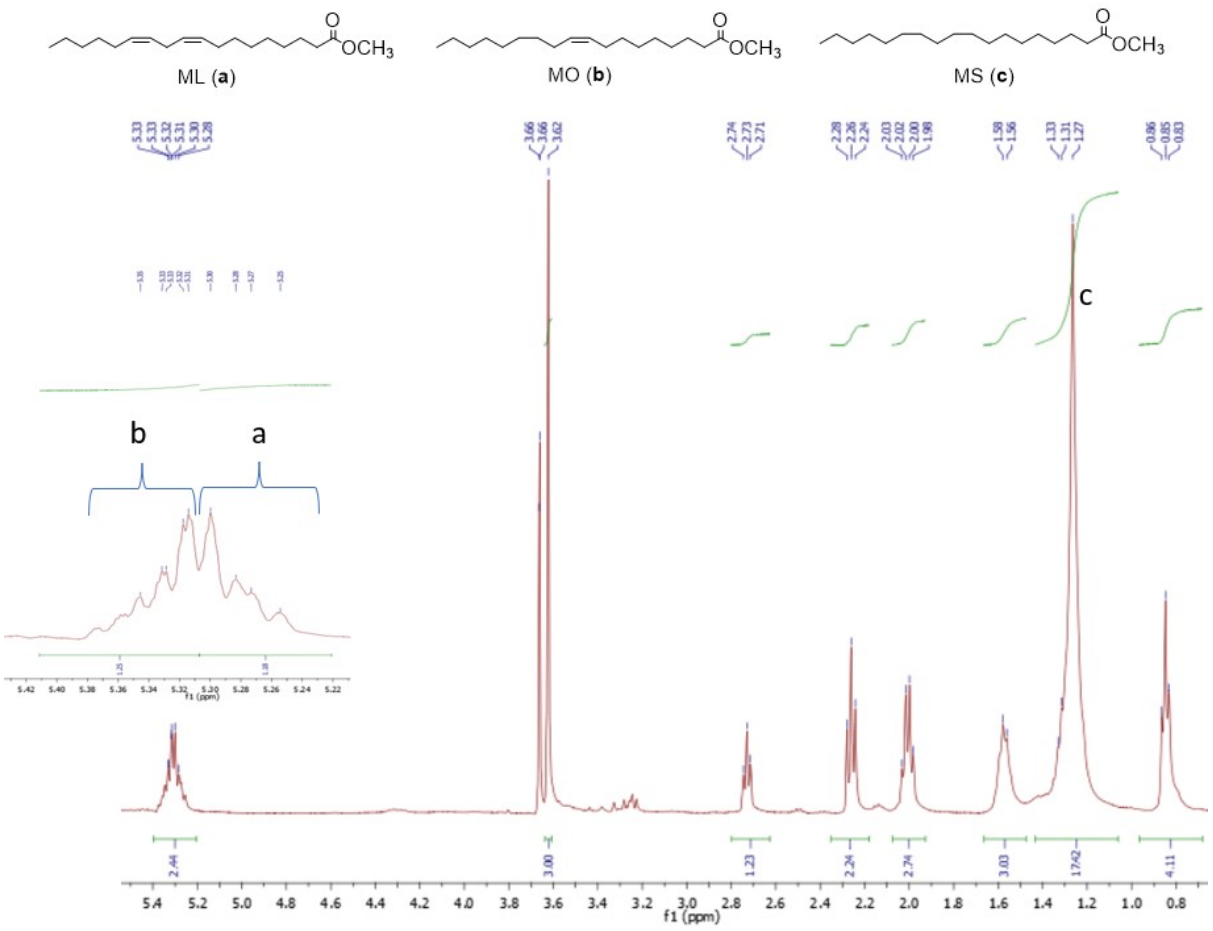


**Fig. S9** $^{1}$H NMR spectrum of products from the hydrogenation of methyl linoleate using complex **2** showing the distribution of the products of the MO and MS at 1 h; 2.5 µmol (0.83 mol%) of the catalyst; 0.3 mmol of methyl linoleate; 5 mL of methanol; 50 °C; 5 bar. 34% conversions; 66% selectivity towards MO;17% selectivity towards MS.

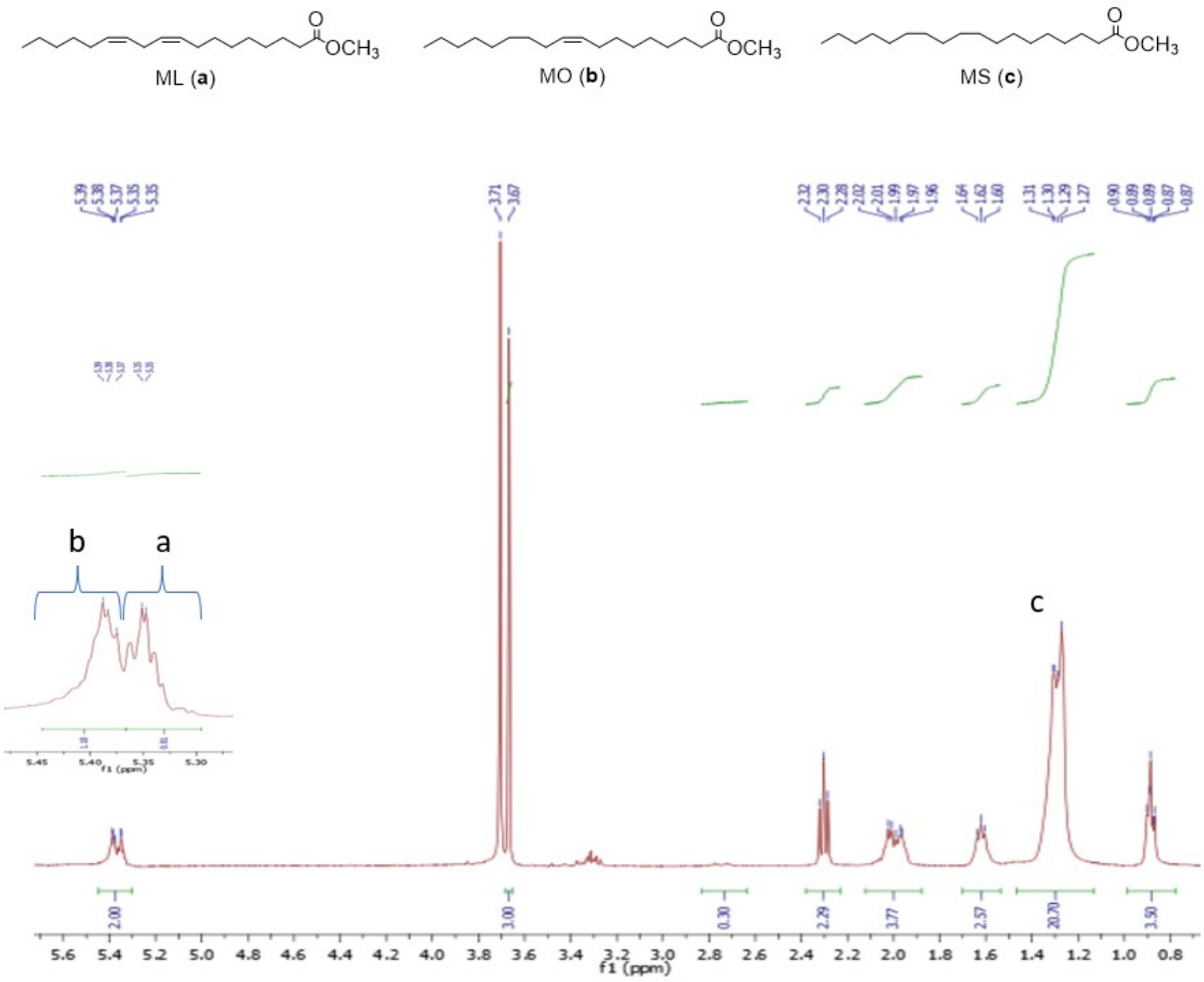


**Fig. S10** $^{1}$H NMR spectrum of products from the hydrogenation of methyl linoleate using complex **2** showing the distribution of the products of MO and MS at 2 h; 2.5 µmol (0.83 mol%) of the catalyst; 0.3 mmol of methyl linoleate; 5 mL of methanol; 50 °C; 5 bar. 46% conversions; 54% selectivity towards MO;16% selectivity towards MS.

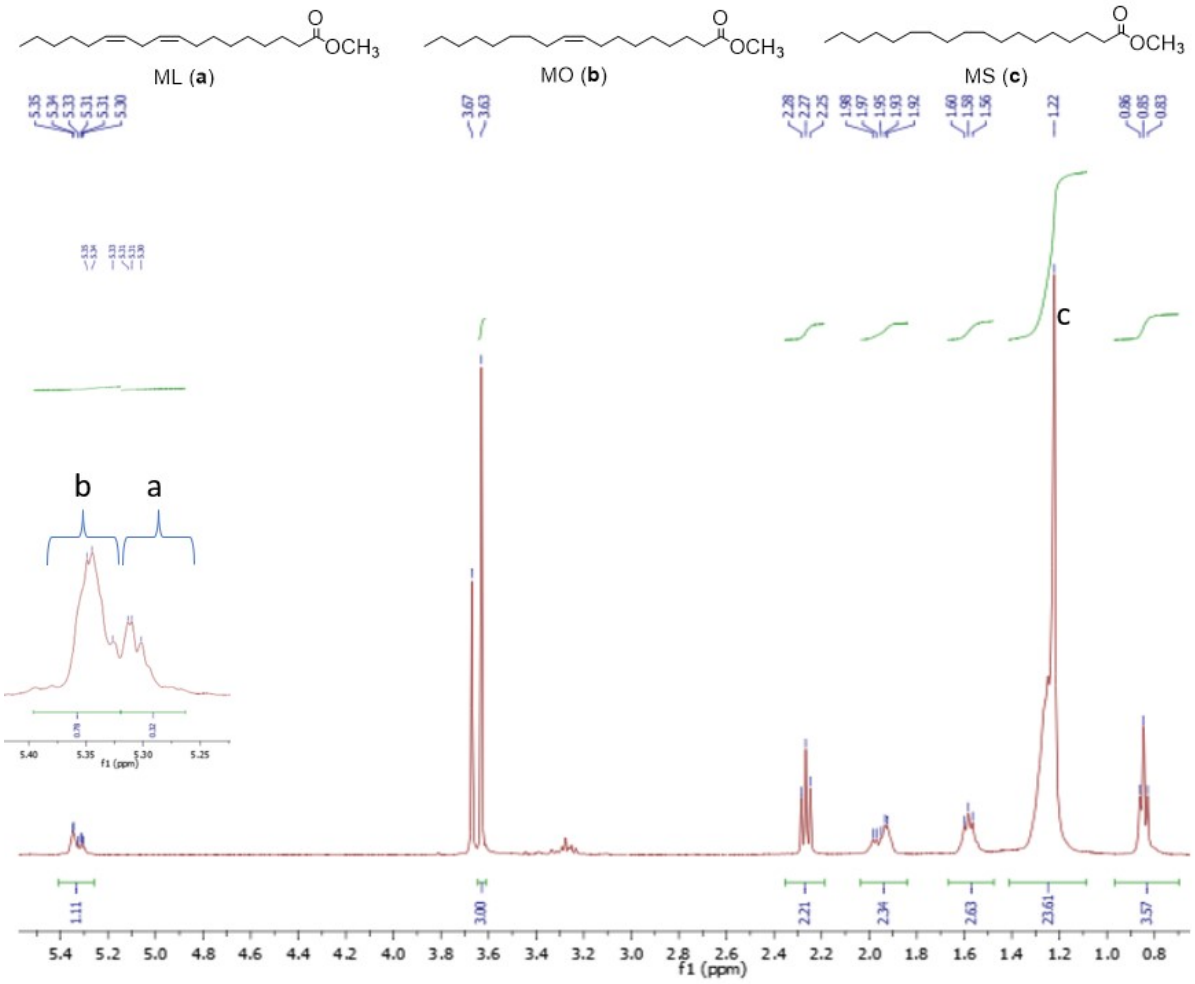


**Fig. S11** $^{1}$H NMR spectrum of products from the hydrogenation of methyl linoleate using complex **6** showing the distribution of the products of MO and MS at 2 h; 2.5 µmol (0.83 mol%) of the catalyst; 0.3 mmol of methyl linoleate; 5 mL of methanol; 50 °C; 5 bar. 70% conversions; 30% selectivity towards MO; 38% selectivity towards MS.

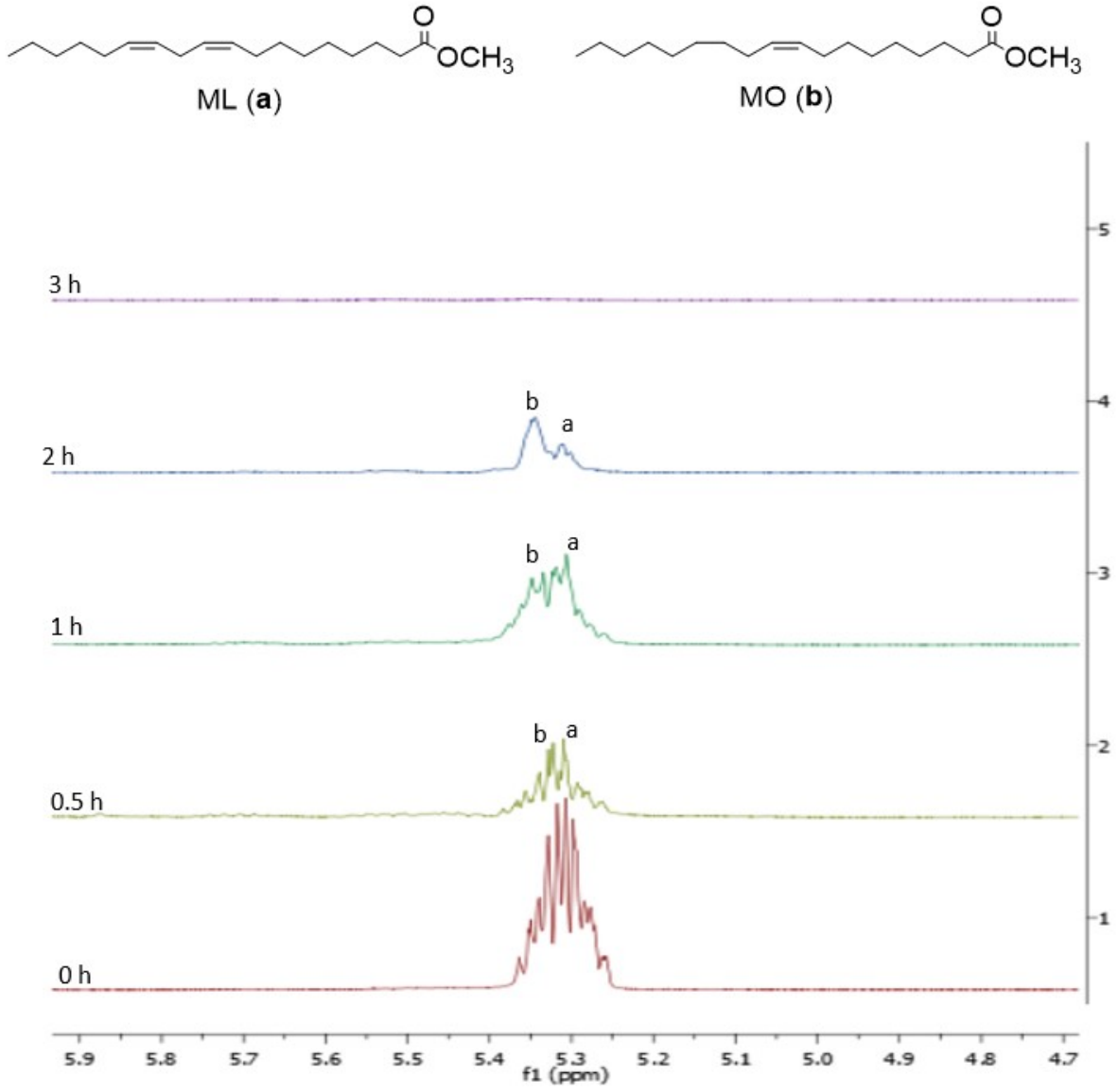


**Fig. S12** $^{1}$H NMR spectrum of a time-dependent study of % conversion of ML and selectivity towards MO with complex **6**. 2.5 µmol (0.83 mol%) of the catalyst; 0.3 mmol of methyl linoleate; 5 mL of methanol; 50 °C; 5 bar.

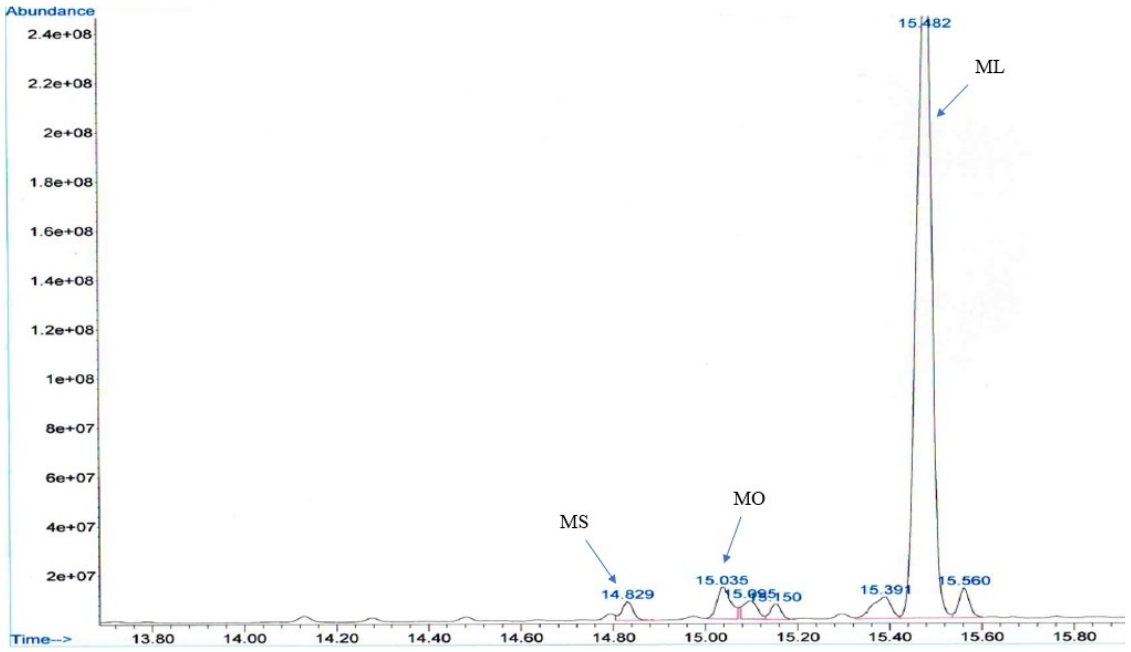


**Fig. S13** The chromatogram showing the distribution of the products of MO and MS for the hydrogenation of methyl linoleate (ML) using complex **6**.

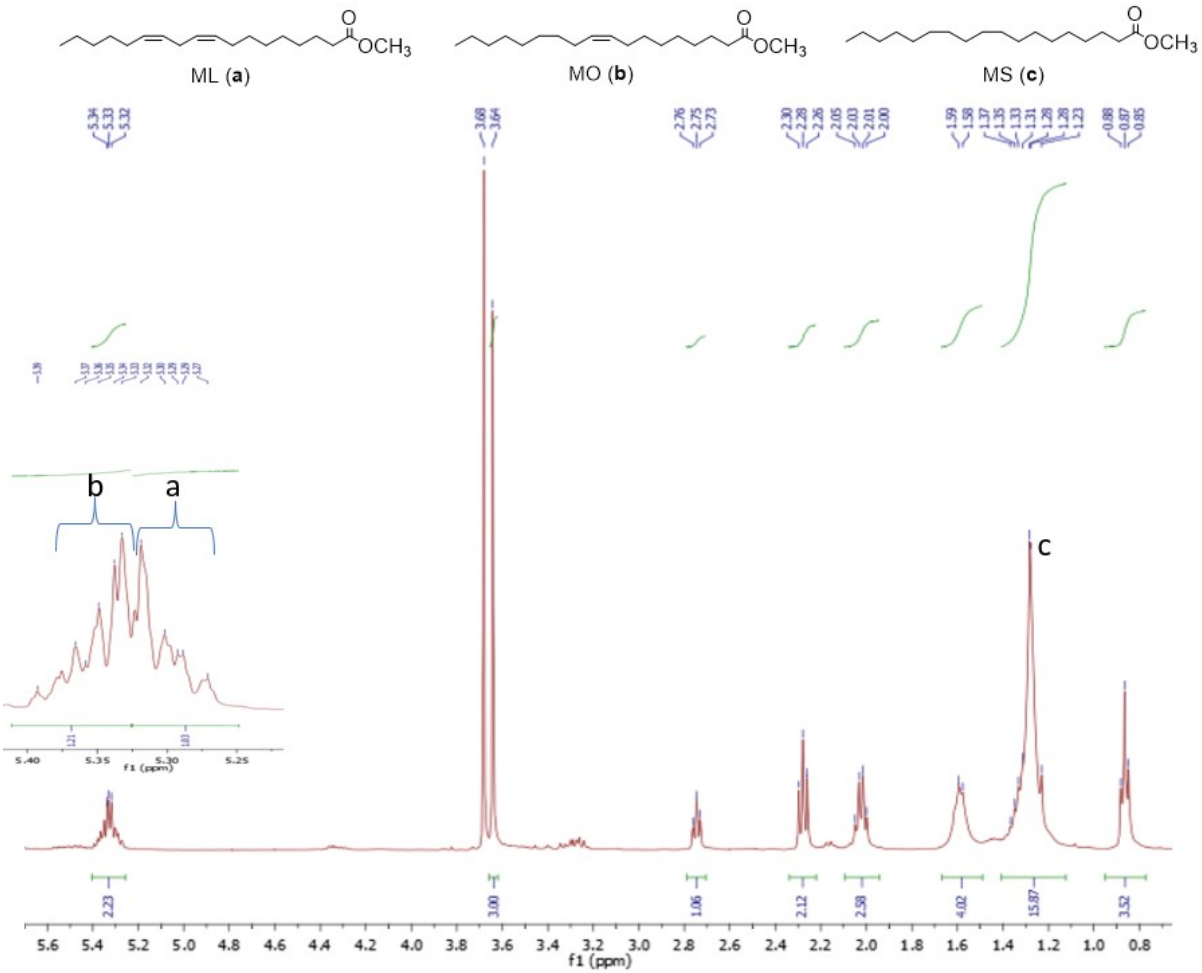


**Fig. S14** $^{1}$H NMR spectrum of products from the hydrogenation of methyl linoleate using complex **3** showing the distribution of the products of MO and MS at 1 h; 2.5 μmol (0.83 mol%) of the catalyst; 0.3 mmol of methyl linoleate; 5 mL of methanol; 50 °C; 5 bar. 40% conversions; 61% selectivity towards MO; 8% selectivity towards MS.

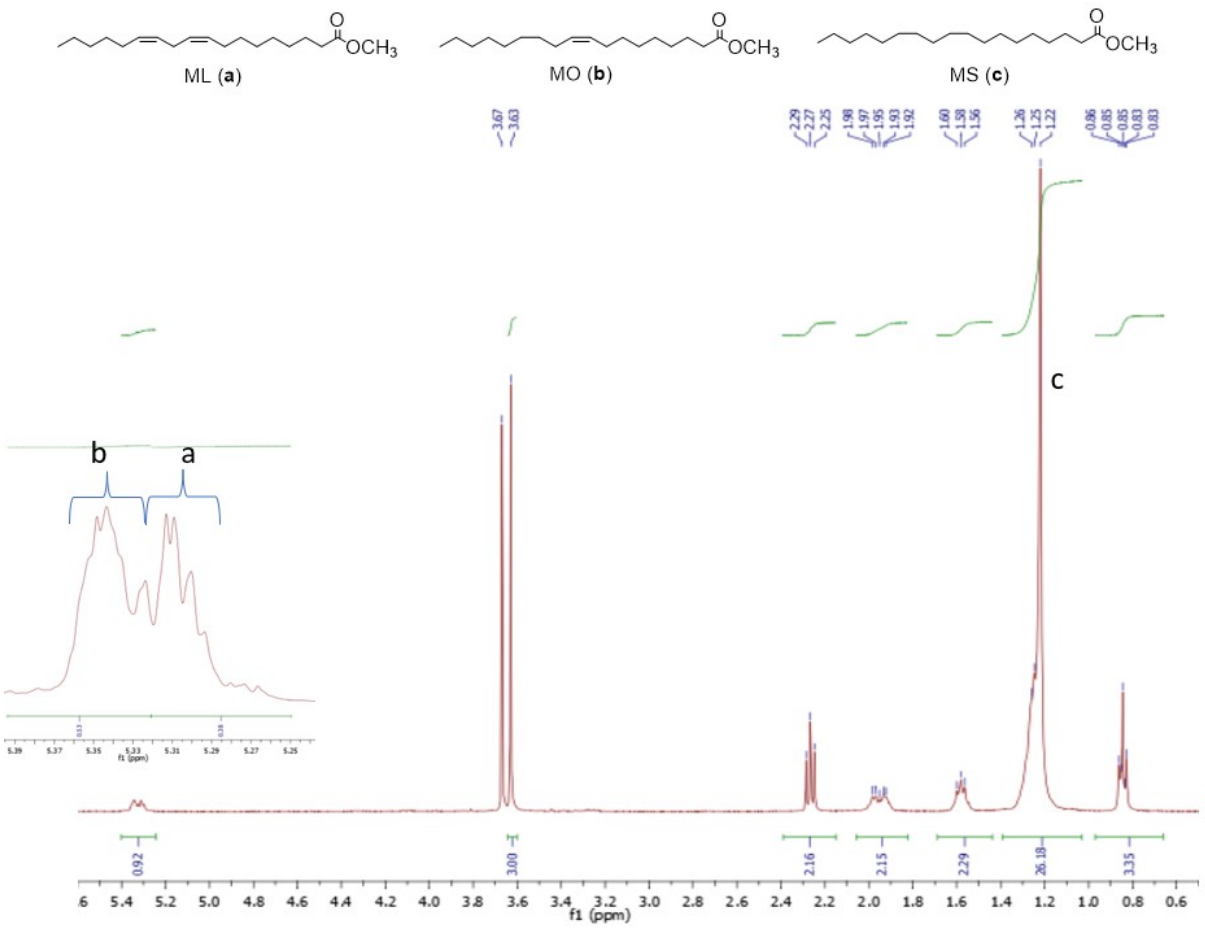


**Fig. S15** $^{1}$H NMR spectrum of products from the hydrogenation of methyl linoleate using complex **3** showing the distribution of the product of MO and MS at 2 h; 2.5 µmol (0.83 mol%) of the catalyst; 0.3 mmol of methyl linoleate; 5 mL of methanol; 50 °C; 5 bar. 75% conversions; 25% selectivity towards MO; 44% selectivity towards MS.

**Table S1** Effect of temperature, pressure, and mercury-drop test on the hydrogenation reaction of methyl linoleate with **6** using molecular hydrogen[a]

| Entry | Complex | $P_{H_2}$ (bar) | Temperature (°C) | Conversion (%) | TON | TOF | Amount of MO detected (%)[b] | Amount of MS detected (%)[b] |
|---|---|---|---|---|---|---|---|---|
| 1 | **6** | 5 | 40 | 17 | 20 | 20 | 83 | 3 |
| 2 | **6** | 5 | 50 | 35 | 42 | 42 | 65 | 21 |
| 3 | **6** | 5 | 60 | 41 | 49 | 49 | 59 | 18 |
| 4 | **6** | 5 | 70 | 36 | 47 | 47 | 64 | 17 |
| 5 | **6** | 10 | 50 | 51 | 61 | 61 | 49 | 34 |
| 6 | **6** | 15 | 50 | 100 | 120 | 120 | fully hydrogenated | |
| 7[c] | **6** | 5 | 50 | 29 | 35 | 35 | 63 | 3 |

[a]Reaction conditions: 2.5 µmol (0.83 mol%) of complex; 0.3 mmol of methyl linoleate; 5 mL of methanol; 50 °C; 5 bar ; 1 h. [b]Conversions were estimated by $^1$H NMR spectroscopy. Each run was performed in duplicates.[c]mercury drop experiment; one equimolar of mercury to complex **6**. $TOF\ in\ mol_{substrate} mol_{catalyst}^{-1} h^{-1}$

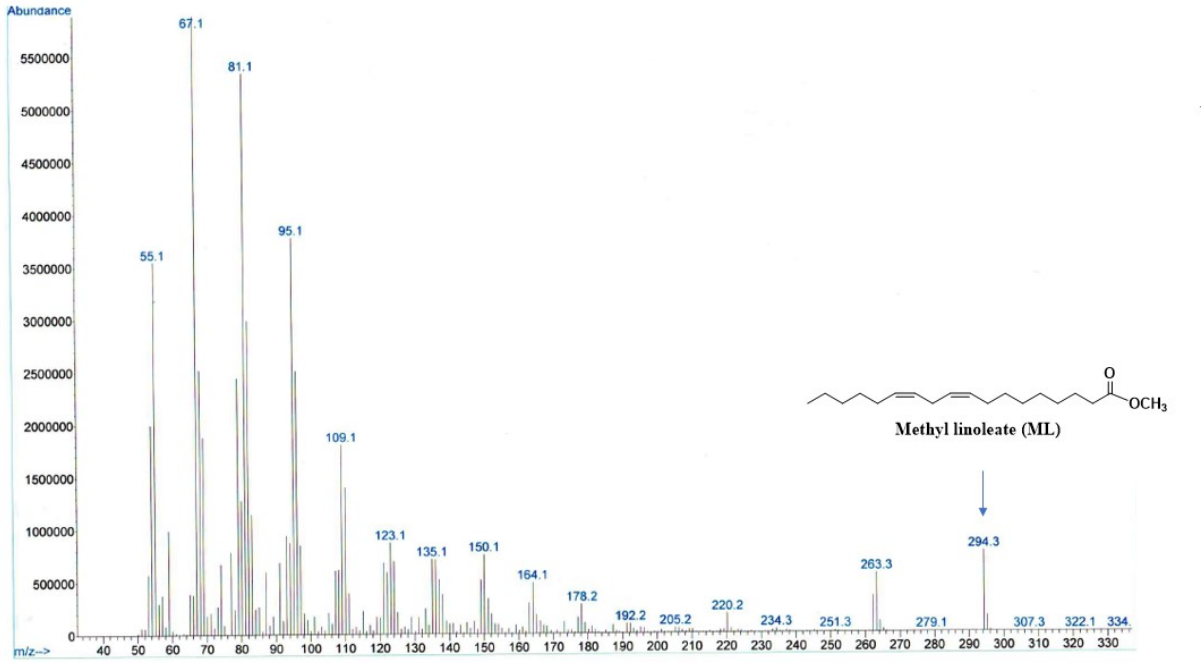


**Fig. S16** The mass spectrum showing the presence of ML when it is not fully hydrogenated with pyrazolyl nickel(II) and palladium(II) complexes.

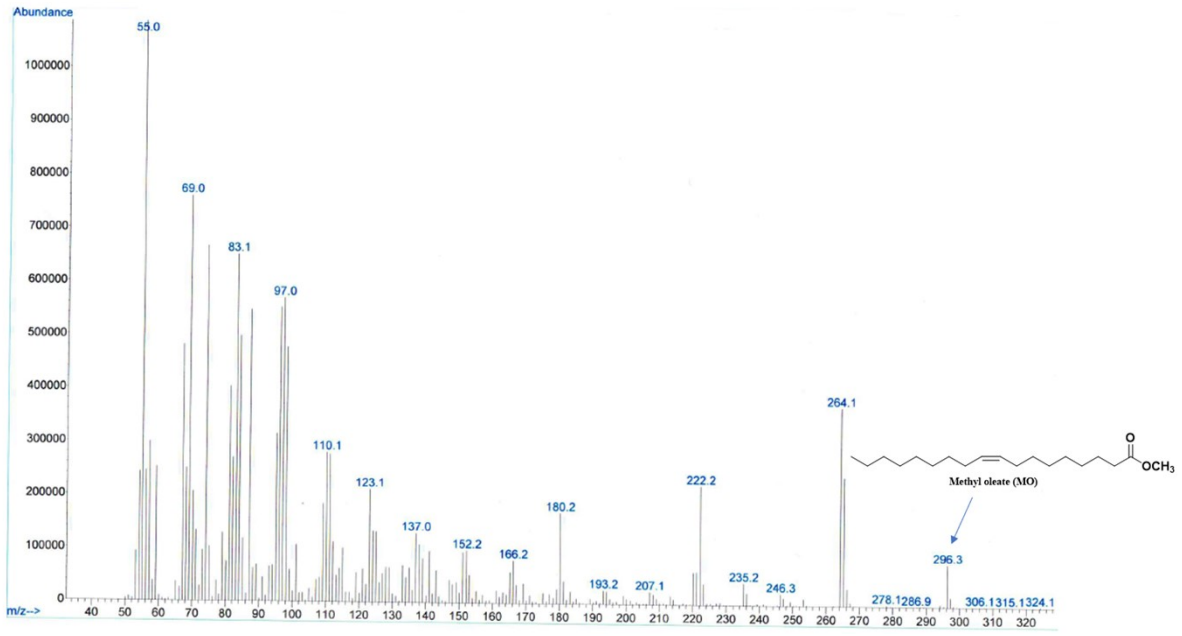


**Fig. S17** The mass spectrum showing the intermediate (MO) when methyl linoleate (ML) is partially hydrogenated.

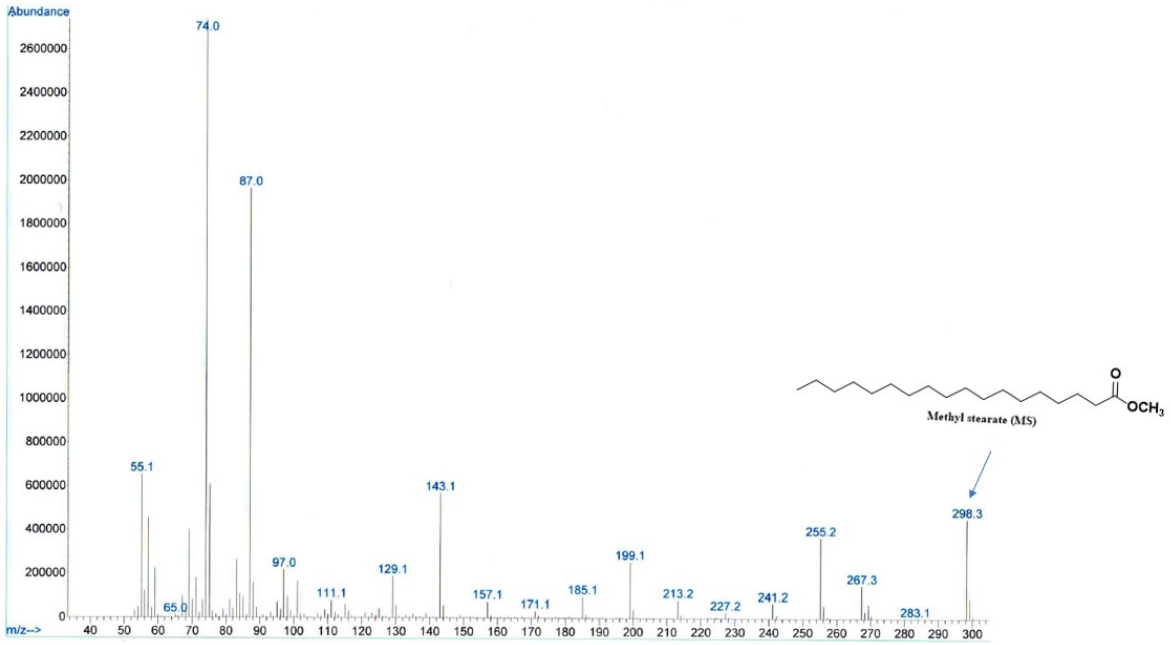


**Fig. S18** The mass spectrum confirming the presence of methyl stearate (MS) when methyl linoleate is fully hydrogenated.

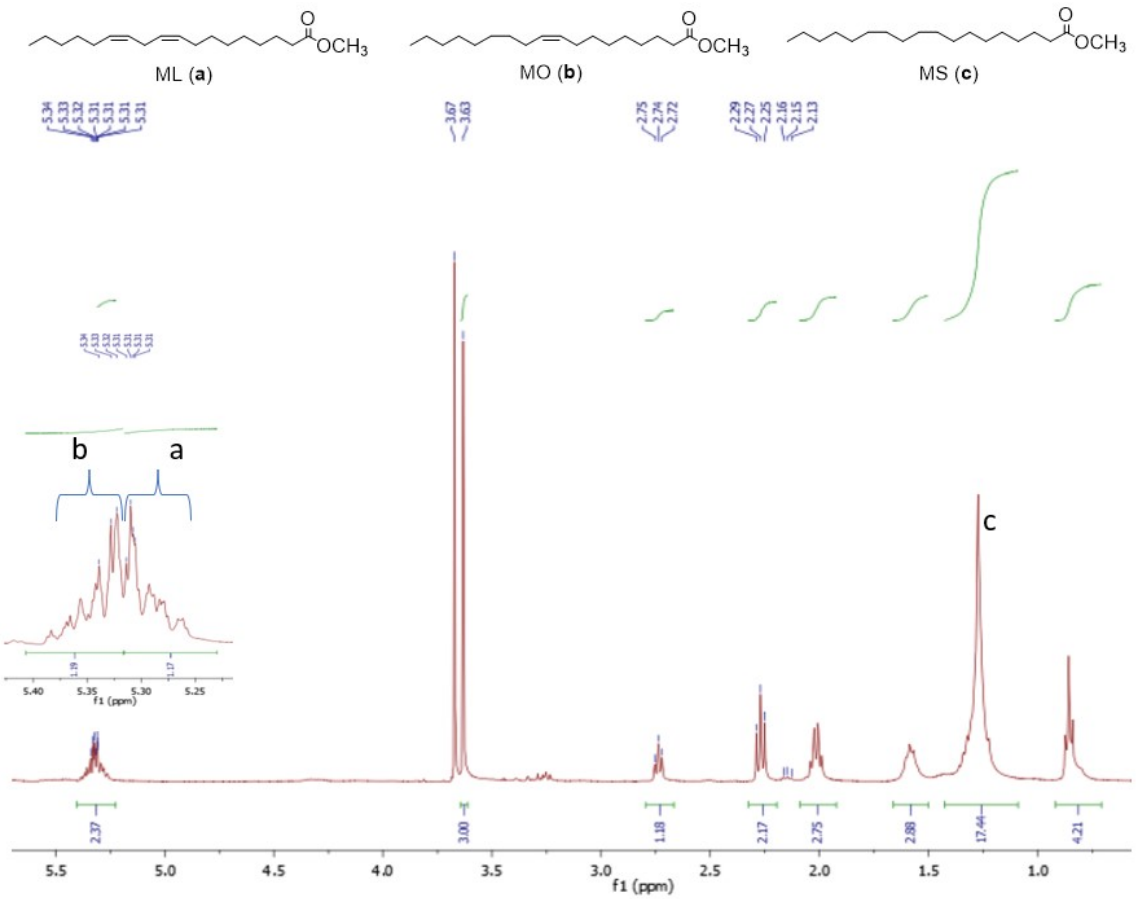


**Fig. S19** $^{1}$H NMR spectrum of products from the hydrogenation of methyl linoleate using complex **6** showing the distribution of the product of MO and MS at 1 h; 2.5 µmol (0.83 mol%) of the catalyst; 0.3 mmol of methyl linoleate; 5 mL of methanol; 70 °C; 5 bar. 36% conversions; 64% selectivity towards MO; 17% selectivity towards MS.

**Fig. S20** $^{1}$H NMR spectrum of products from the hydrogenation of methyl linoleate (ML) using complex **6** showing the distribution of the products of MO and MS. 2.5 μmol (0.83 mol%) of the catalyst; 0.5 mg of Hg; 0.3 mmol of methyl linoleate; 5 mL of methanol; 50 °C; 5 bar, 1 h. 29% conversion; 71% selectivity towards MO and 3% selectivity towards MS.

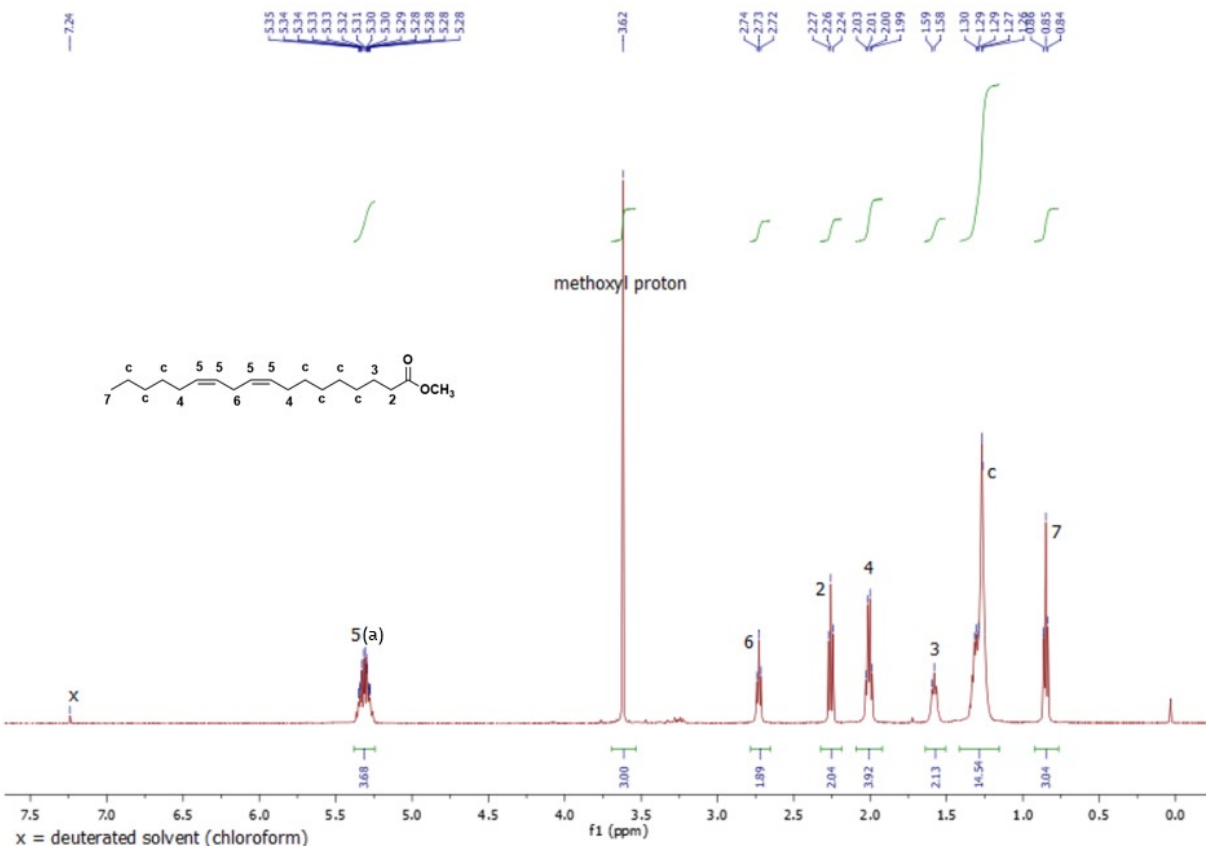


| Peaks | Integration (ppm) |
|---|---|
| 5 (a) | 3.68 |
| 6 | 1.89 |
| c | 14.54 |

**Fig. S21** A representation of $^{1}$H NMR spectrum for the hydrogenation of methyl linoleate (ML). 2.5 µmol (0.83 mol%) of the catalyst; 0.3 mmol of methyl linoleate; 5 mL of methanol; 50 °C; 5 bar.

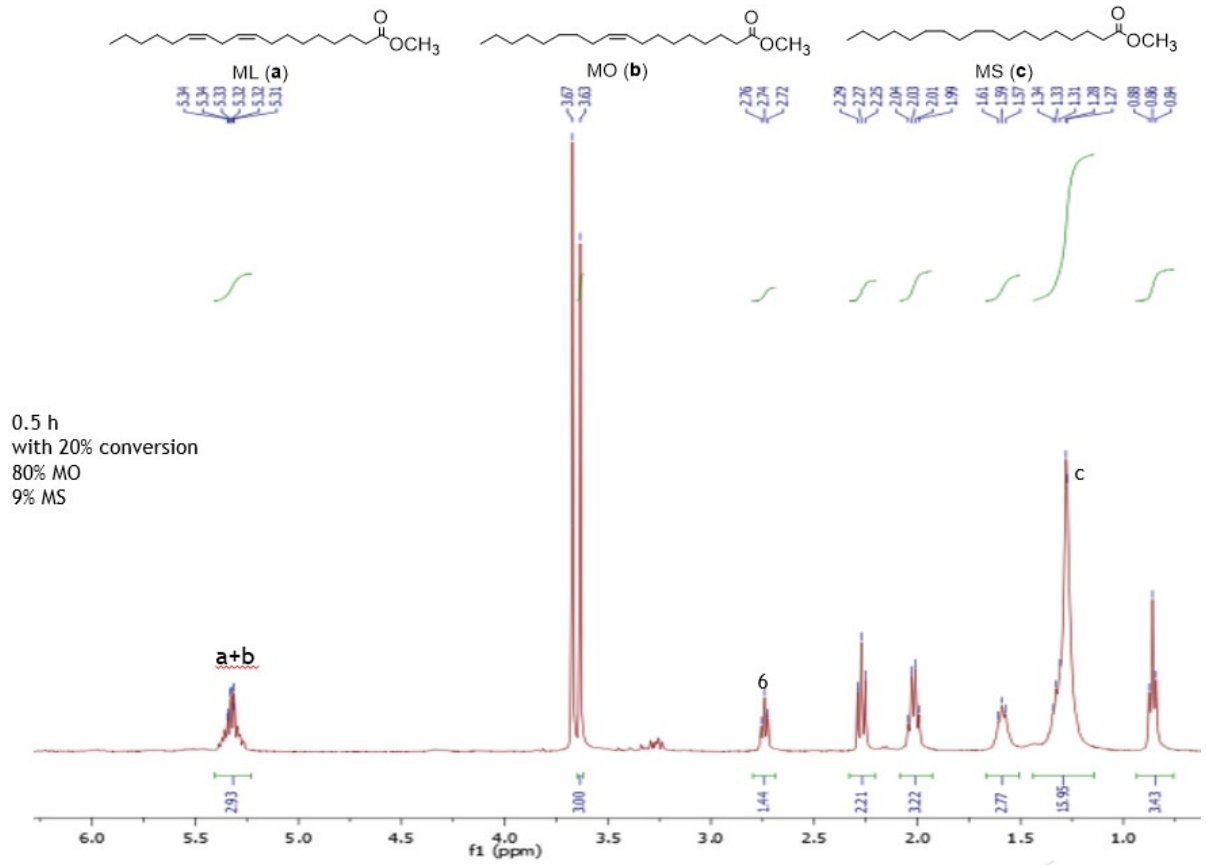


Hint:

| Peaks | Integration (ppm)(0.5 h) |
|---|---|
| 5 (a+b) | 3.68 (2.93) |
| 6 | 1.89 (1.44) |
| c | 14.54 (15.95) |

% conversion = ((3.68 -2.93)/3.68 ) x 100 % = 20%
MO selectivity = (2.93/3.68) x 100% = 80%
MS selectivity = ((15.95-14.54)/15.95) x 100% = 8.8%

**Fig. S22** A representation of $^{1}$H NMR spectrum for the hydrogenation of methyl linoleate(ML). 2.5 µmol (0.83 mol%) of the catalyst; 0.3 mmol of methyl linoleate; 5 mL of methanol; 50 °C; 5 bar.

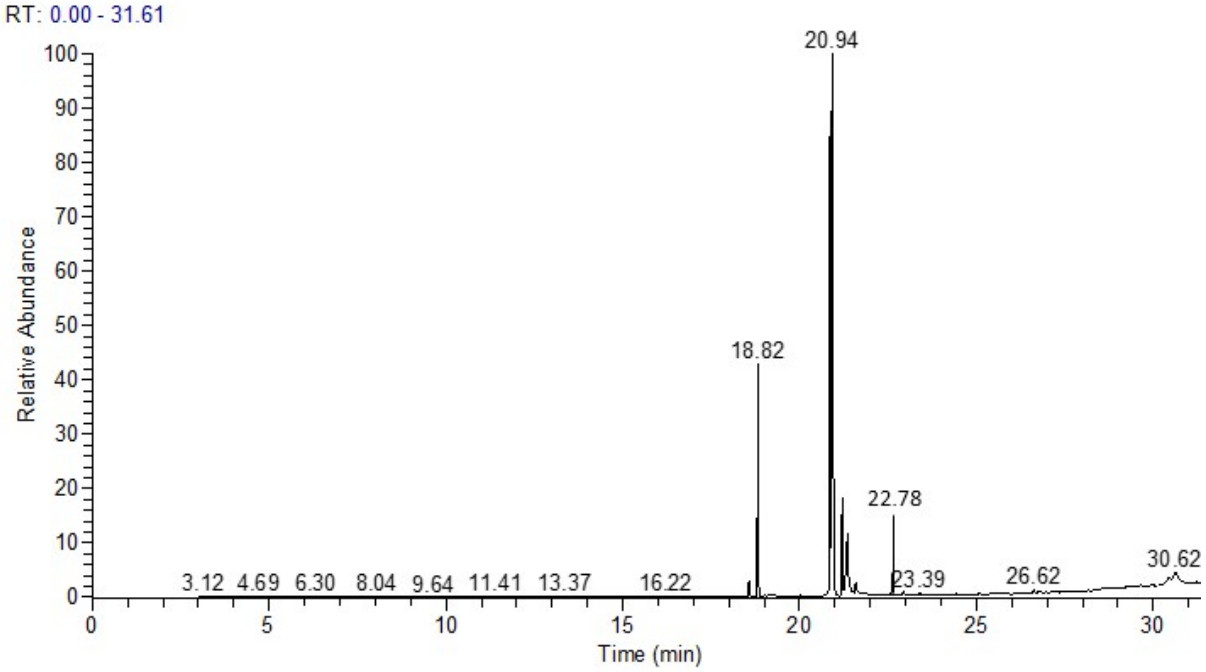


| RT(min) | Peak Area | Area % |
|---|---|---|
| 18.82 (C16:0) | 4395247020.48 | 14.1 |
| 20.86 (C18:2) | 9776445645.15 | 31.4 |
| 20.94 (C18:1) | 11426610037.23 | 36.7 |
| 21.21 (C18:0) | 1805840278.34 | 5.8 |
| 21.35 (oleic acid) | 1158228592.09 | 3.7 |
| 22.78 (C18:3) | 1650164392 | 5.3 |

**Fig. S23** Methyl ester composition of biodiesel produced from jatropha seed oil.

$$Ester\ (FAME)\ content\ (\%) = \frac{\sum (peak\ area\ of\ ester\ (FAME)}{\sum (peak\ areas\ of\ all\ compounds)}\ x\ 100$$

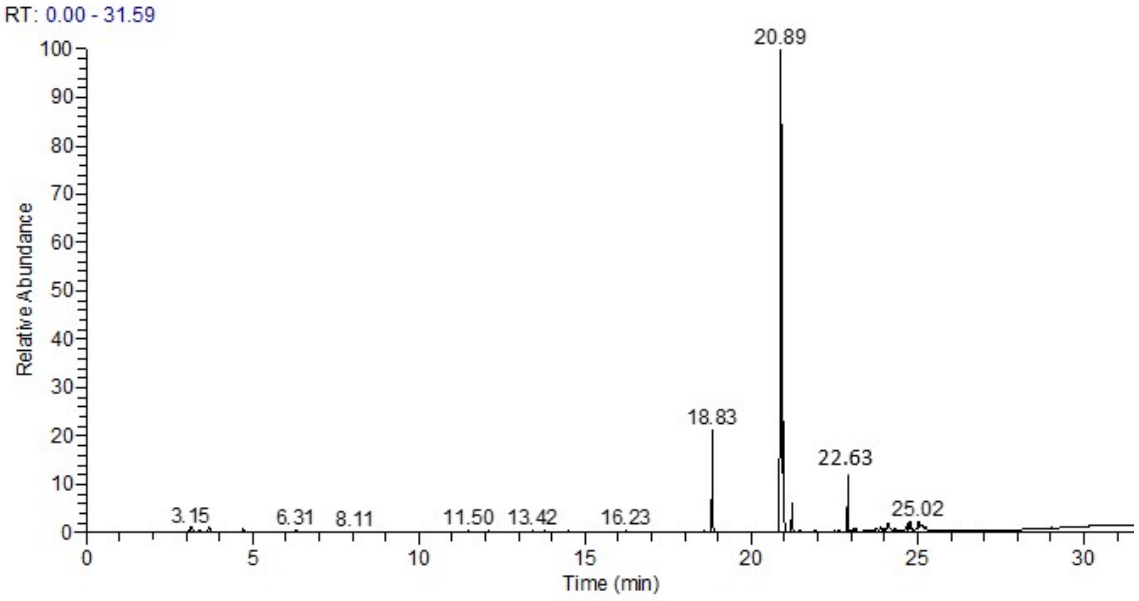


| RT (min) | Peak Area | Area % |
|---|---|---|
| 18.83 (C16:0) | 3003110510.97 | 9.3 |
| 20.94 (C18:1) | 50377988.73 | 0.2 |
| 20.89 (C18:2) | 24745639658 | 76.9 |
| 21.22 (C18:0) | 970175730.51 | 3.0 |
| 22.63 (C18:3) | 2509358391.23 | 7.8 |

**Fig. S24** Methyl ester composition of biodiesel produced from chinaberry seed oil.

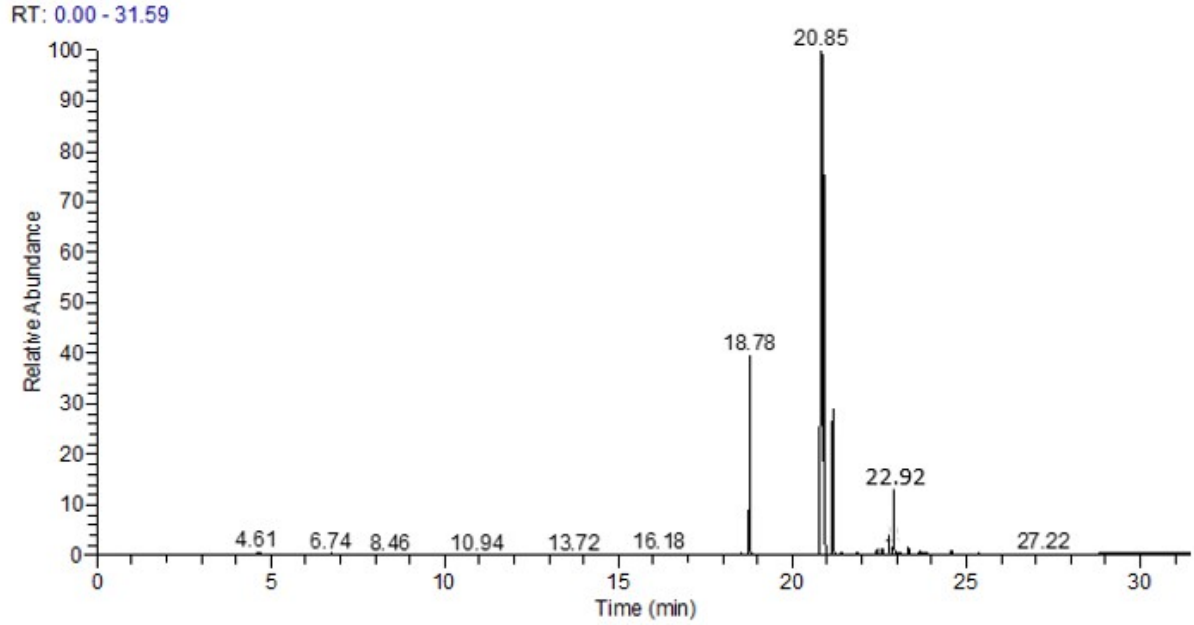


| RT (min) | Peak Area | Area % |
|---|---|---|
| 18.78 (C16:0) | 6378956906.56 | 13.0 |
| 20.85 (C18:2) | 23487629868.3 | 47.7 |
| 22.62 (C18:1) | 11134665720.01 | 22.6 |
| 21.16 (C18:0) | 5510876526.26 | 11.2 |
| 22.92 (C18:3) | 2120410520.12 | 4.3 |

**Fig. S25** Methyl ester composition of biodiesel produced from *tsamma* melon seed oil.

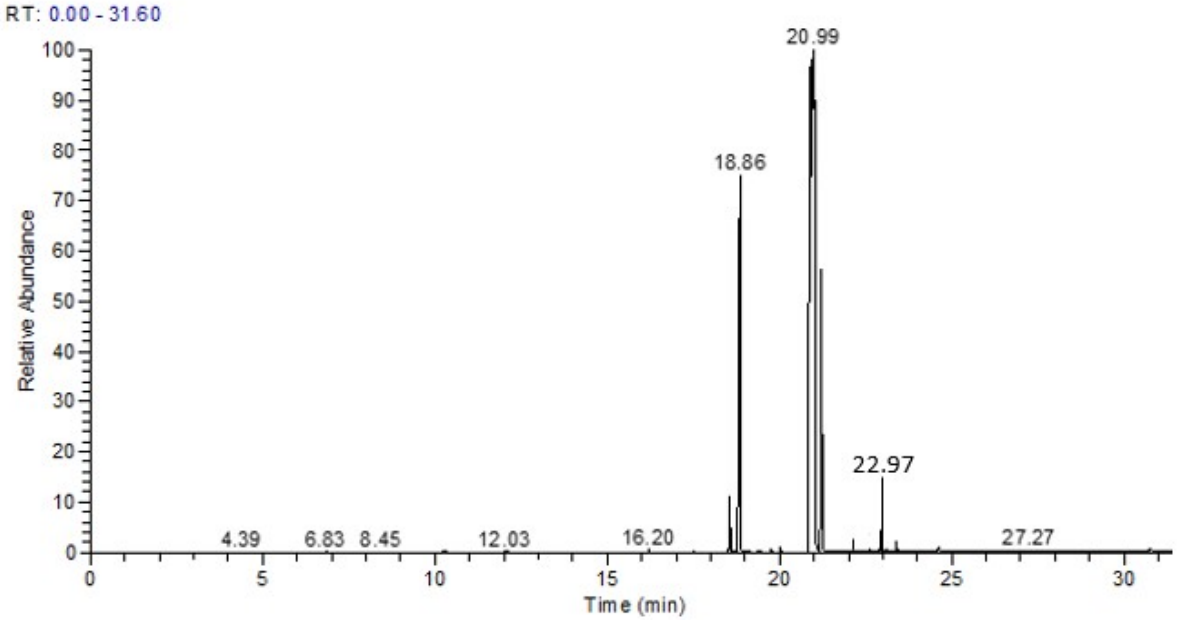


| RT (min) | Peak Area | Area % |
|---|---|---|
| 20.92 (C18:2) | 37642520212 | 23.3 |
| 20.99 (C18:1) | 60421899395.9 | 37.4 |
| 21.22 (C18:0) | 9047129321.3 | 5.6 |
| 22.97 (C18:3) | 2423338211.1 | 1.5 |

**Fig. S26** Product distribution for the jatropha methyl esters with complex **2**. 8.6 µmol of the complex (1 wt.%); 0.5 g of JBH; 10 mL of methanol; 50 °C; 10 bar; 1 h.

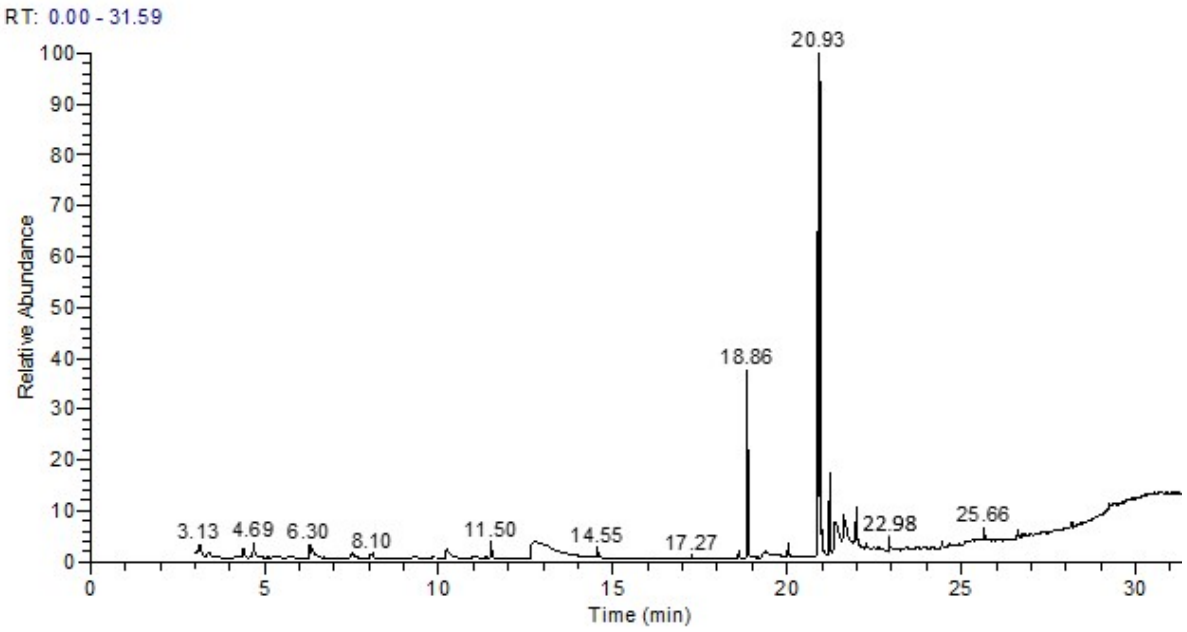


| RT (min) | Peak Area | Area % |
|---|---|---|
| 20.87 (C18:2) | 639396689.5 | 21.3 |
| 20.93 (C18:1) | 1007812034.13 | 33.6 |
| 21.22 (C18:0) | 162167727.06 | 5.4 |
| 22.98 (C18:3) | 29995048.3 | 1.0 |

**Fig. S27** Product distribution for the jatropha methyl esters with complex **2**. 8.6 μmol of the complex (1 wt.%); 0.5 g of JBH; 10 mL of methanol; 50 °C; 10 bar; 2 h.

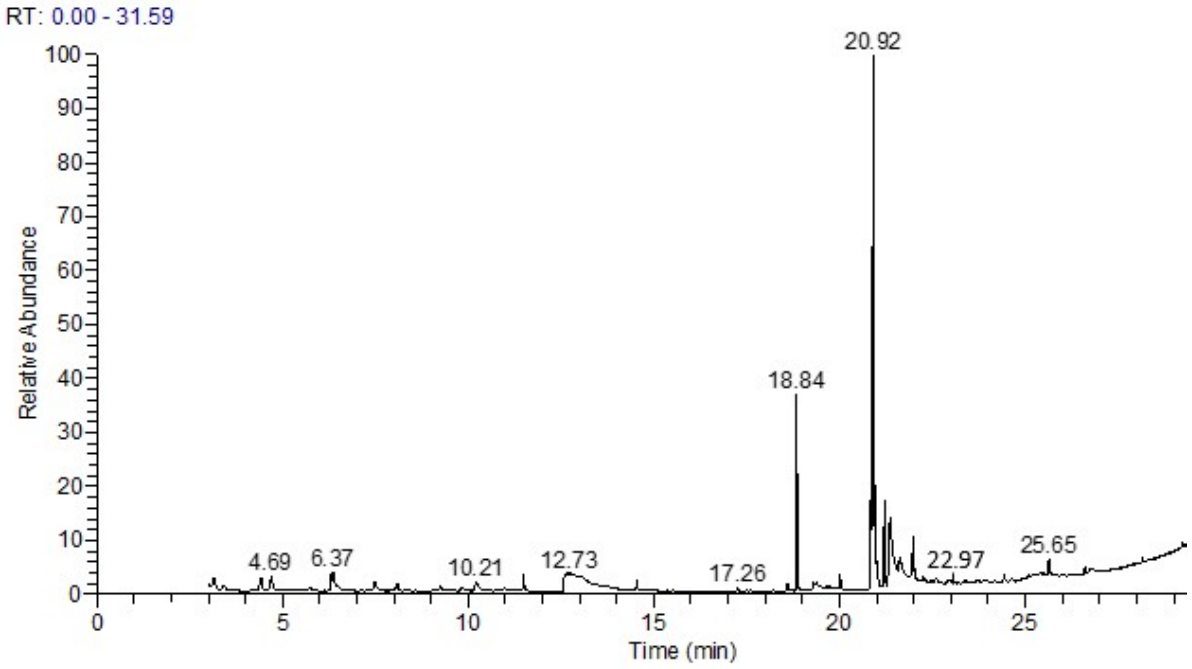


| RT (min) | Peak Area | Area % |
|---|---|---|
| 20.86 (C18:2) | 622592884.4 | 20.1 |
| 20.92 (C18:1) | 938535542.2 | 30.3 |
| 21.21 (C18:0) | 213725915.6 | 6.9 |
| 22.97 (C18:3) | 15487385.19 | 0.5 |

**Fig. S28** Product distribution for the jatropha methyl esters with complex **2**. 8.6 μmol of the complex (1 wt.%); 0.5 g of JBH; 10 mL of methanol; 50 °C; 10 bar; 3 h.

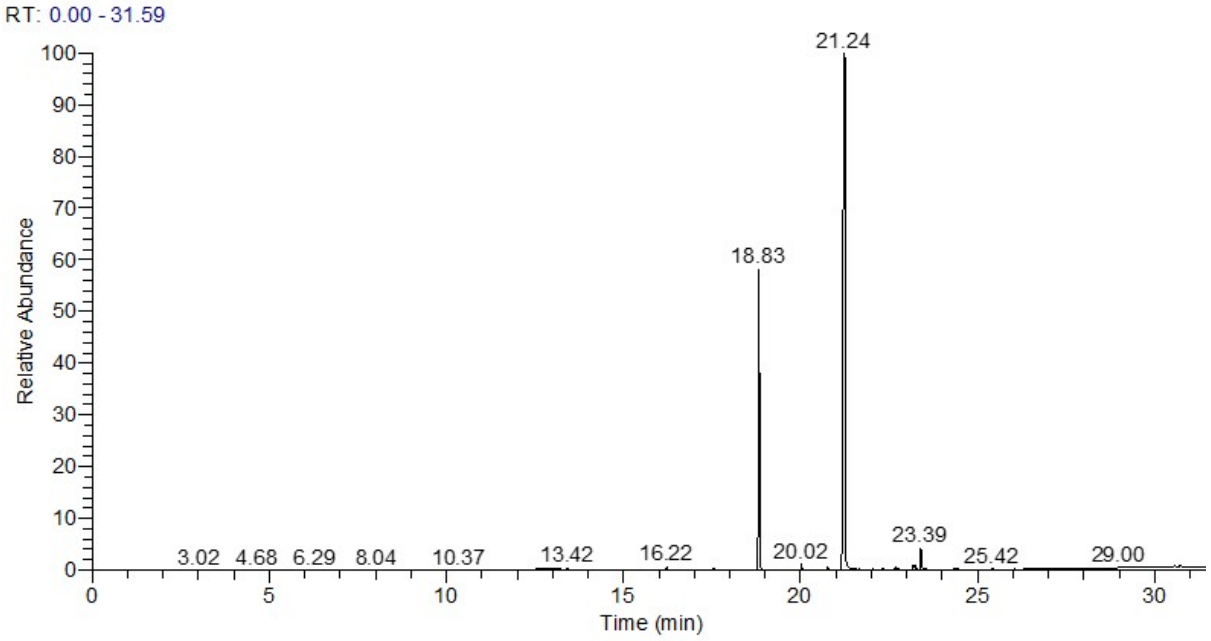


| RT (min) | Peak Area | Area % |
|---|---|---|
| 20.87 (C18:2) | - | - |
| 20.98 (C18:1) | 25852864.77 | 0.05 |
| 21.24 (C18:0) | 36870718361 | 75.2 |
| 22.98 (C18:3) | - | - |

**Fig. S29** Product distribution for the jatropha methyl esters with complex **2**. 8.6 μmol of the complex (1 wt.%); 0.5 g of JBH; 10 mL of methanol; 50 °C; 10 bar; 4 h.

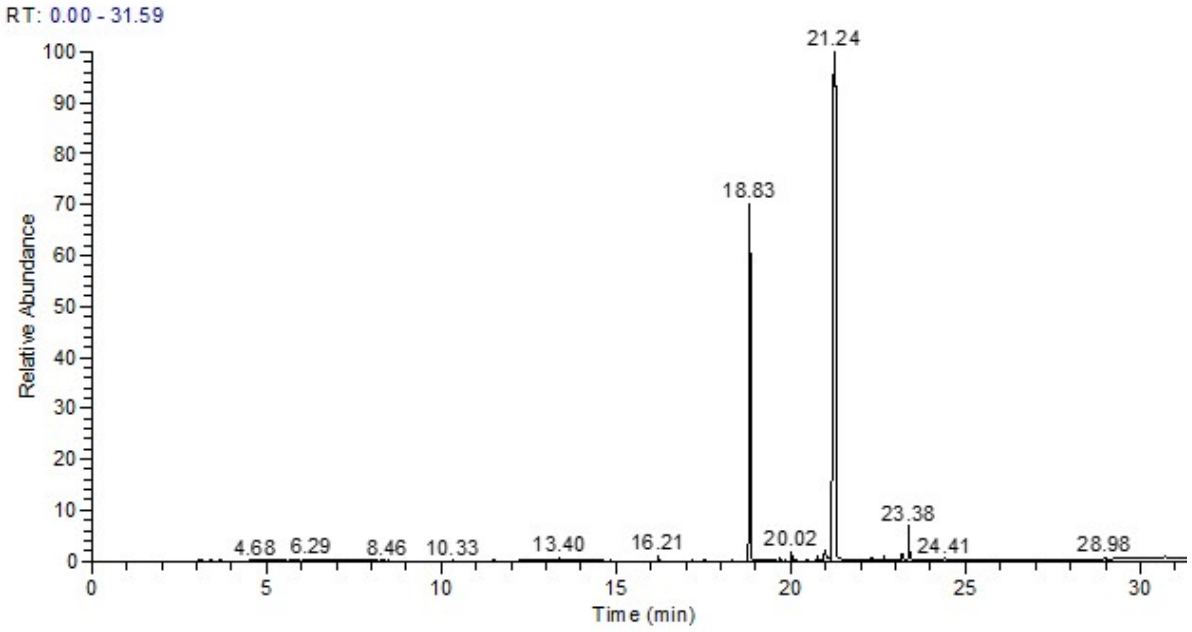


| RT(min) | Peak Area | Area % |
|---|---|---|
| 20.87 (C18:2) | - | - |
| 20.98 (C18:1) | 626416098.6 | 0.94 |
| 21.24 (C18:0) | 48595618197 | 73.4 |
| 22.98 (C18:3) | - | - |

**Fig. S30** Product distribution for the jatropha methyl esters with complex **5**. 8.6 μmol of the complex (1 wt.%); 0.5 g of JBH; 10 mL of methanol; 50 °C; 10 bar; 0.5 h.

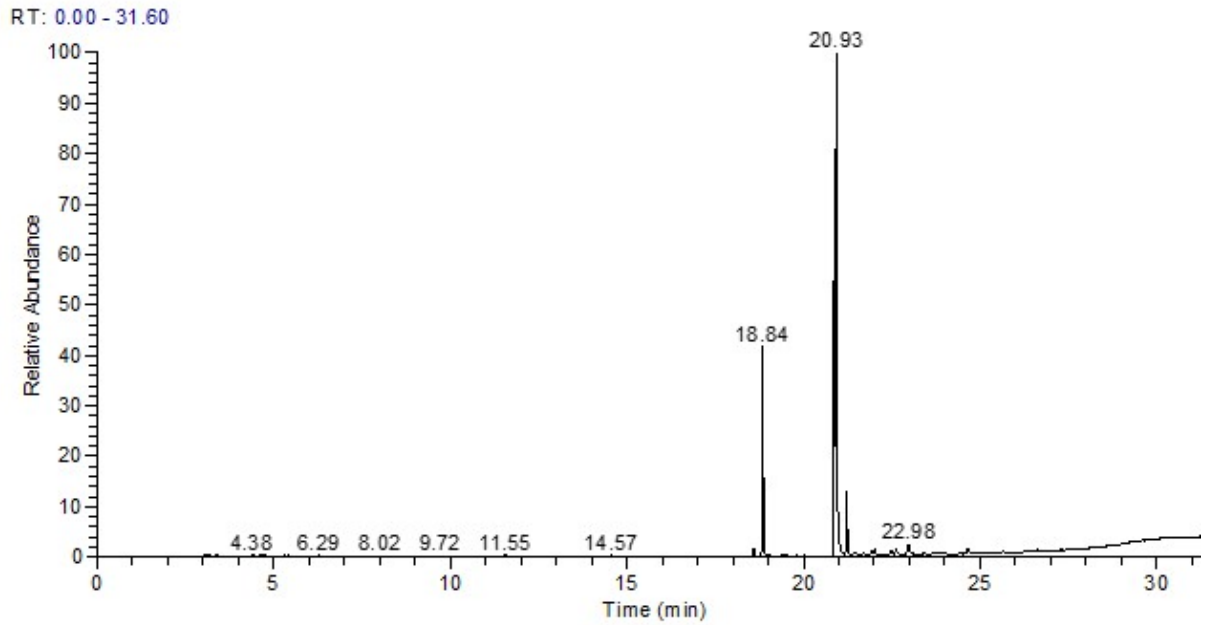


| RT (min) | Peak Area | Area % |
|---|---|---|
| 20.93 (C18:1) | 2359920030.4 | 41.0 |
| 20.87 (C18:2) | 1513802360.3 | 26.2 |
| 21.22 (C18:0) | 592857958.6 | 10.3 |
| 22.98 (C18:3) | 28779512.56 | 0.5 |

**Fig. S31** Product distribution for the jatropha methyl esters with complex **5**. 8.6 μmol of the complex (1 wt.%); 0.5 g of JBH; 10 mL of methanol; 25 °C; 10 bar; 0.5 h.

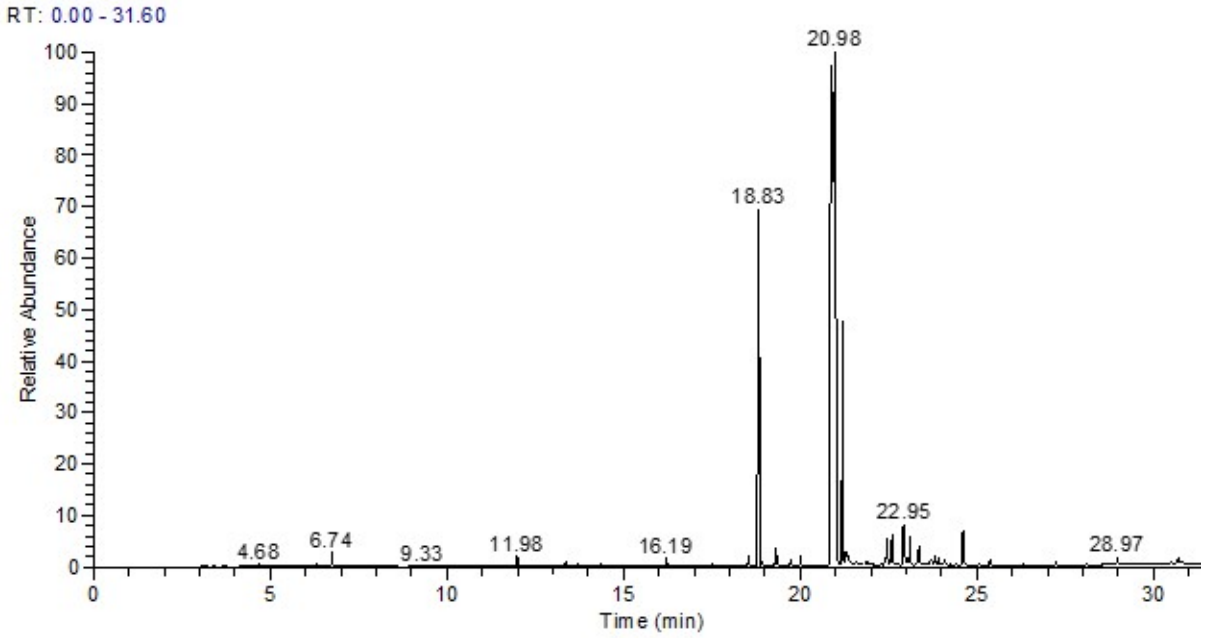


| RT (min) | Peak Area | Area % |
|---|---|---|
| 20.87 (C18:2) | 60139183718.2 | 41.0 |
| 20.98 (C18:1) | 59230440000.1 | 40.4 |
| 21.20 (C18:0) | 7183895033.3 | 4.9 |
| 22.95 (C18:3) | 6450844519.5 | 4.4 |

**Fig. S32** Product distribution for the chinaberry methyl esters with complex **2**. 8.6 μmol of the complex (1 wt.%); 0.5 g of JBH; 10 mL of methanol; 50 °C; 10 bar; 0.5 h.

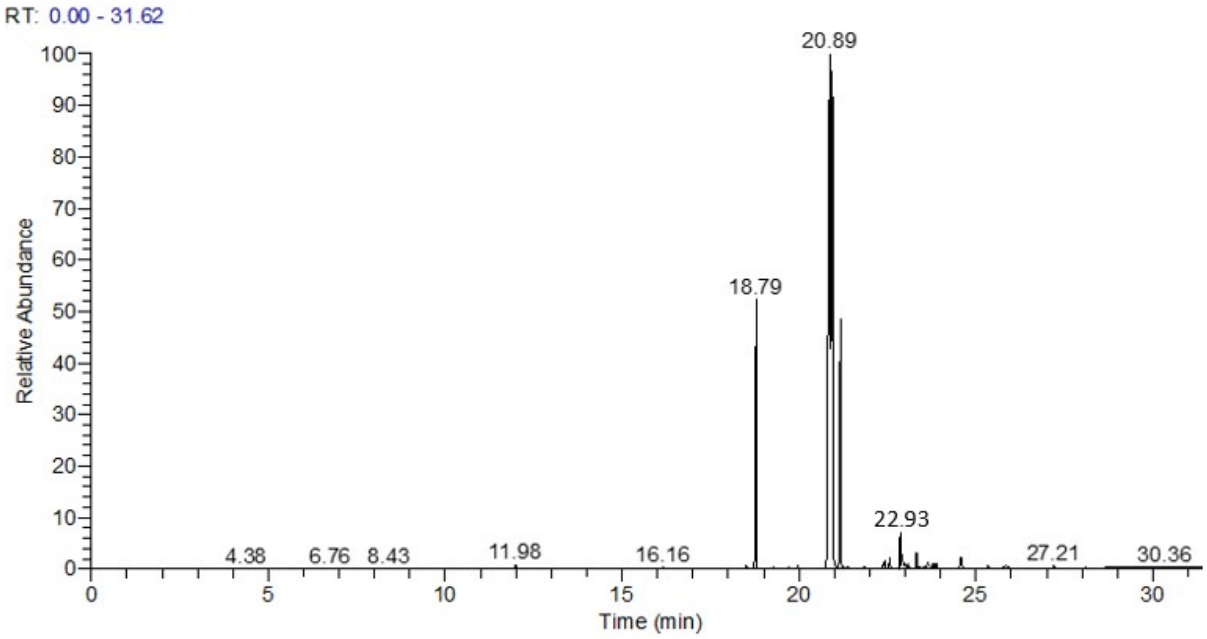


| RT (min) | Peak Area | Area % |
|---|---|---|
| 20.87 (C18:2) | 37575995688.08 | 36.1 |
| 20.89 (C18:1) | 41947718178.23 | 40.3 |
| 21.17 (C18:0) | 14572408300.34 | 14.0 |
| 22.93 (C18:3) | 2810393029.42 | 2.7 |

**Fig. S33** Product distribution for the *tsamma* melon methyl esters with complex **2**. 8.6 µmol of the complex (1 wt.%); 0.5 g of JBH; 10 mL of methanol; 50 °C; 10 bar; 1 h.

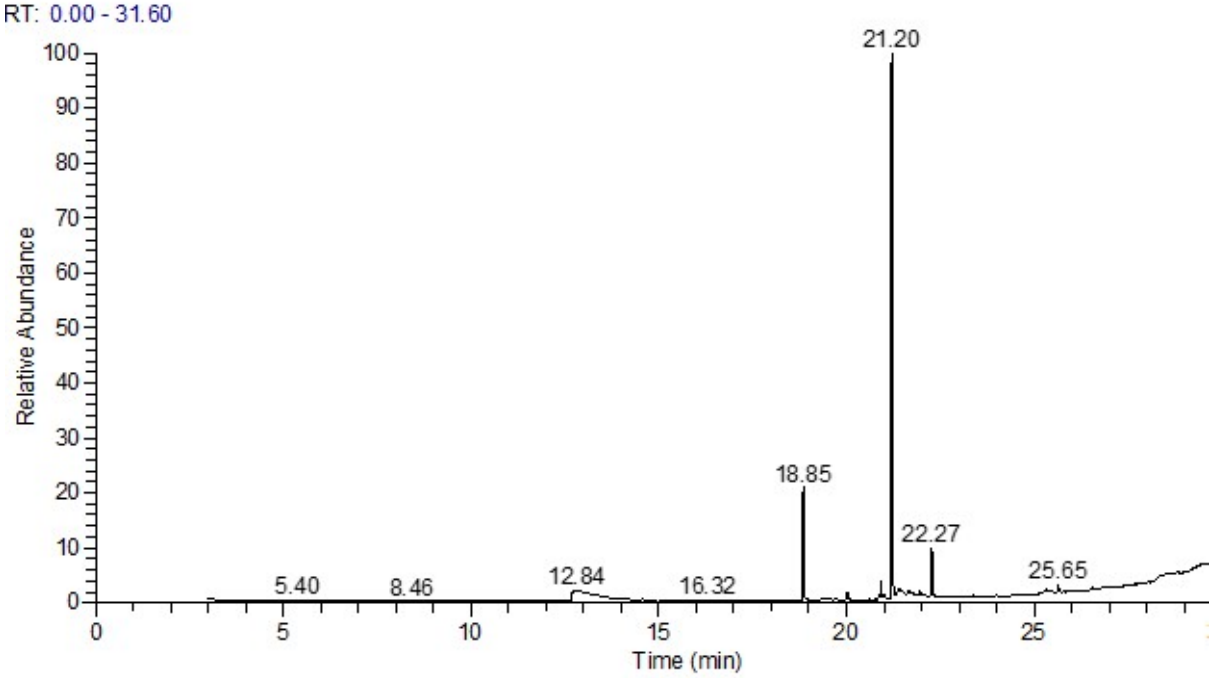


| RT (min) | Peak Area | Area % |
|---|---|---|
| 20.85 (C18:2) | - | - |
| 20.99 (C18:1) | 152306809.8 | 5.8 |
| 21.20 (C18:0) | 1746385918.64 | 66.5 |
| 22.96 (C18:3) | - | - |

**Fig. S34** Product distribution for the chinaberry methyl esters with complex **5**. 8.6 μmol of the complex (1 wt.%); 0.5 g of JBH; 10 mL of methanol; 50 °C; 10 bar; 0.5 h.

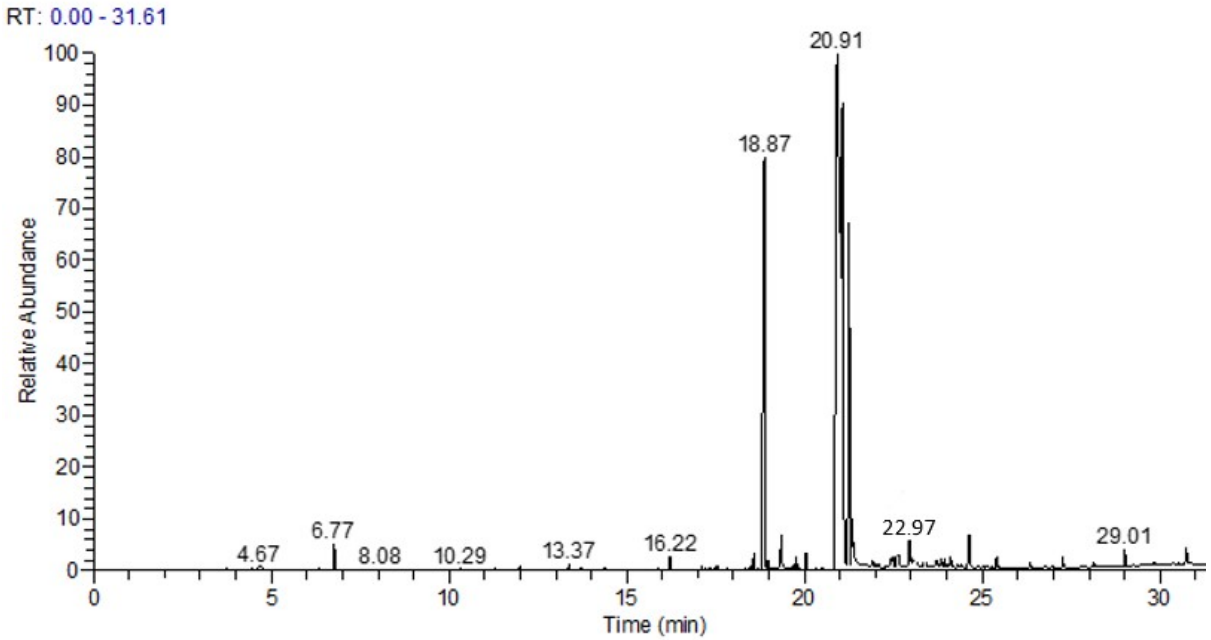


| RT (min) | Peak Area | Area % |
|---|---|---|
| 20.91 (C18:2) | 54795563299.05 | 30.9 |
| 21.06 (C18:1) | 41673001214.49 | 23.5 |
| 21.25 (C18:0) | 25713128408.94 | 14.5 |
| 22.97 (C18:3) | 1418655360.49 | 0.8 |

**Fig. S35** Product distribution for the chinaberry methyl esters with complex **5**. 8.6 μmol of the complex (1 wt.%); 0.5 g of JBH; 10 mL of methanol; 25 °C; 10 bar; 0.5 h.

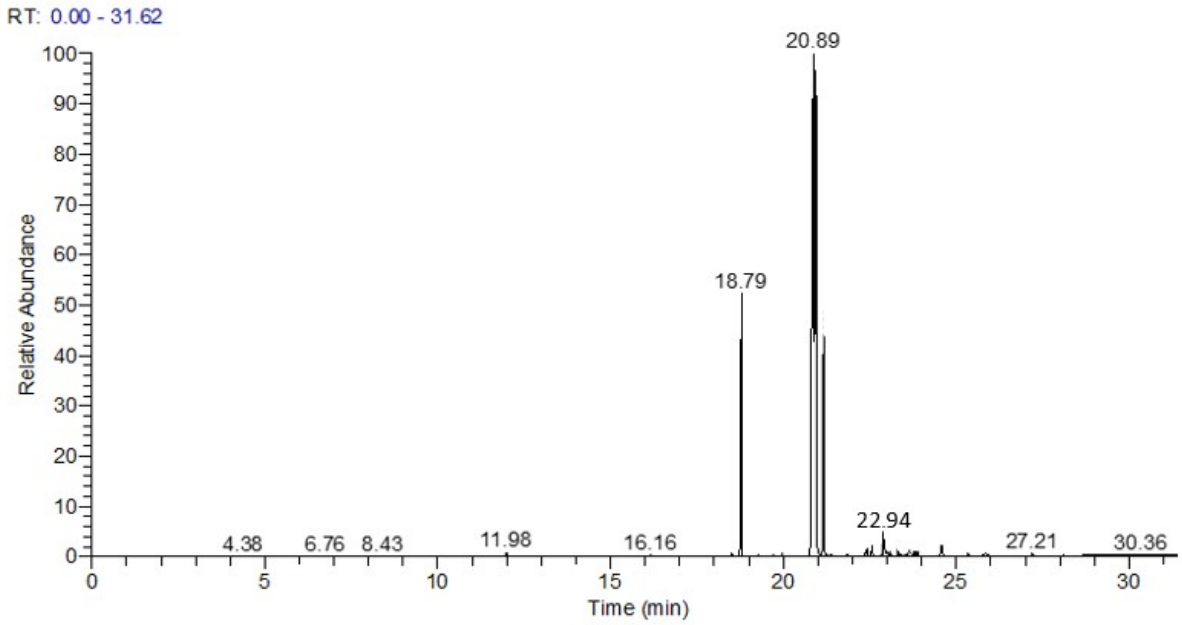


| RT (min) | Peak Area | Area % |
|---|---|---|
| 20.89 (C18:2) | 37888261580.37 | 36.4 |
| 20.91 (C18:1) | 21025903404.12 | 20.2 |
| 21.19 (C18:0) | 17695067221.76 | 16.6 |
| 22.94 (C18:3) | 936797676.4 | 0.9 |

**Fig. S36** Product distribution for the *tsamma* melon methyl esters with complex **5**. 8.6 µmol of the complex (1 wt.%); 0.5 g of JBH; 10 mL of methanol; 25 °C; 10 bar; 0.5 h.

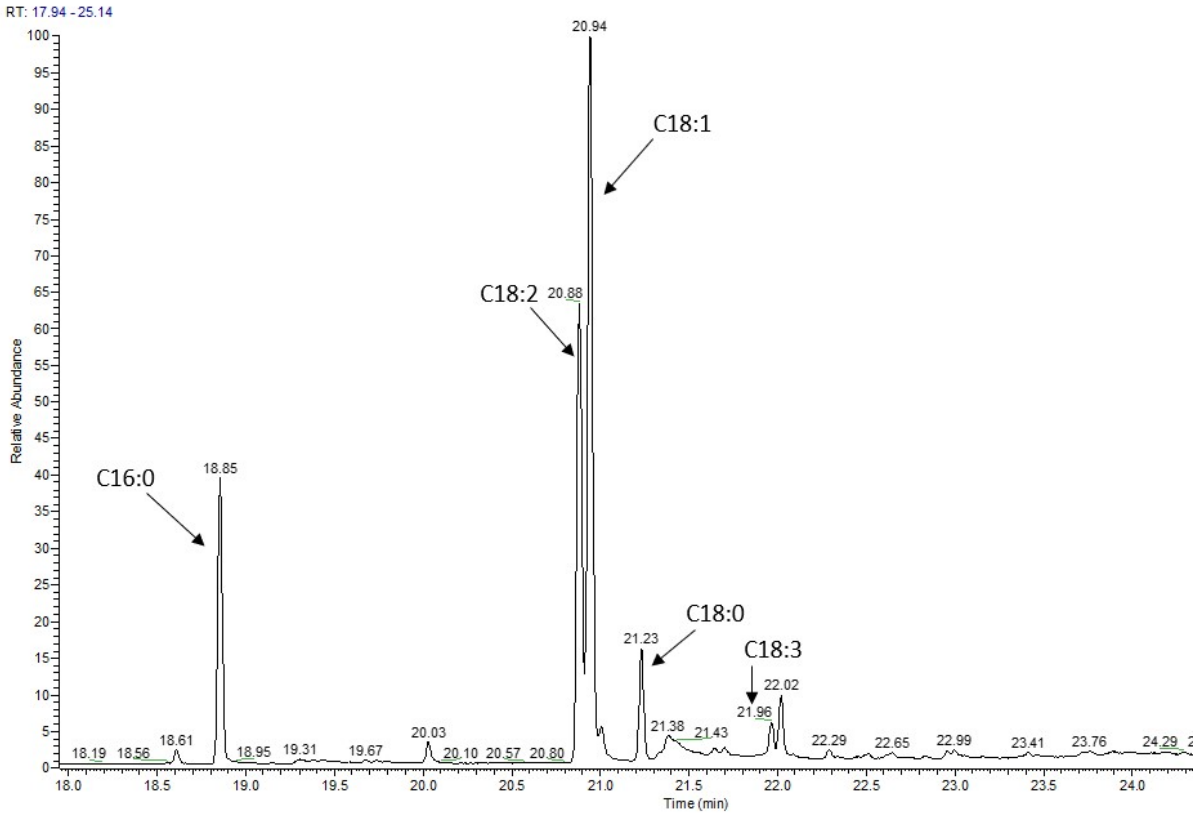


**Fig. S37** Representative gas chromatogram for the partial hydrogenation of biodiesel produced from *Jatropha curcas*, chinaberry (*Melia azedarach*) and *tsamma* melon (*Citrullus ecirrhosus*) seed oils.

*The following are the $^{1}H$ and $^{13}C\{^{1}H\}$ NMR spectra of the palladium complexes used in this study:*

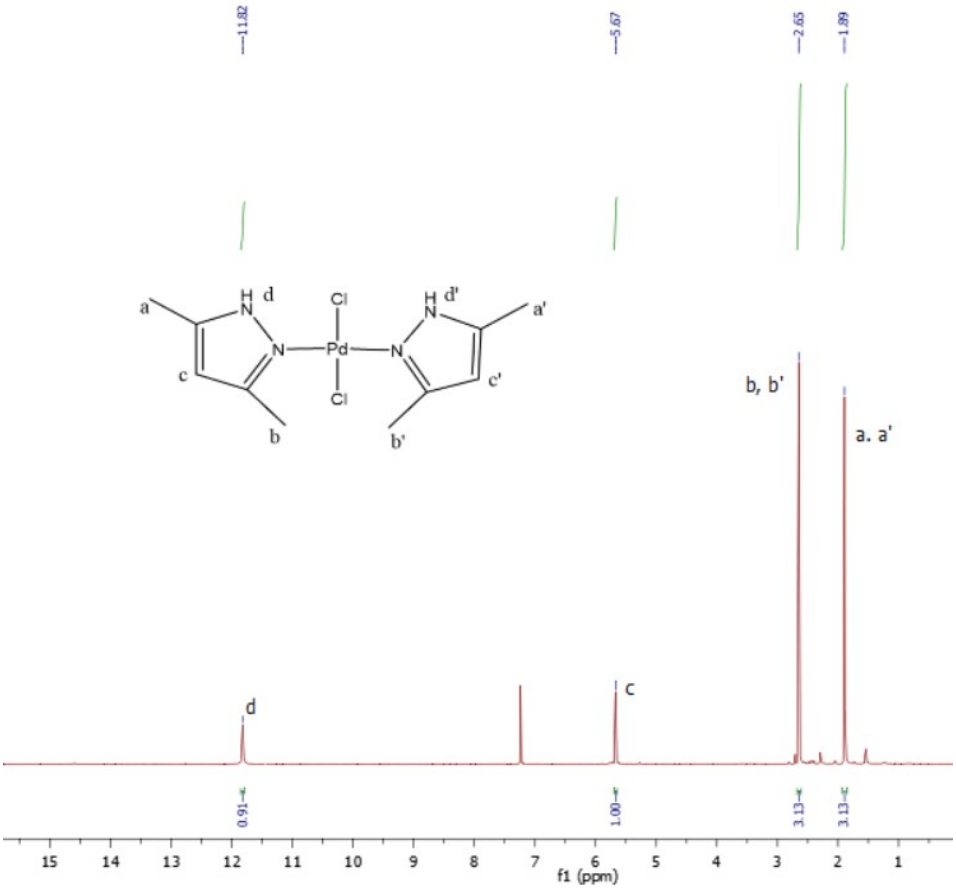


**Fig. S38** $^{1}H$ NMR spectrum of **4** recorded in $CDCl_3$.


**Fig. S39** $^{13}C\{^{1}H\}$ NMR spectrum of **4** recorded in $CDCl_3$.

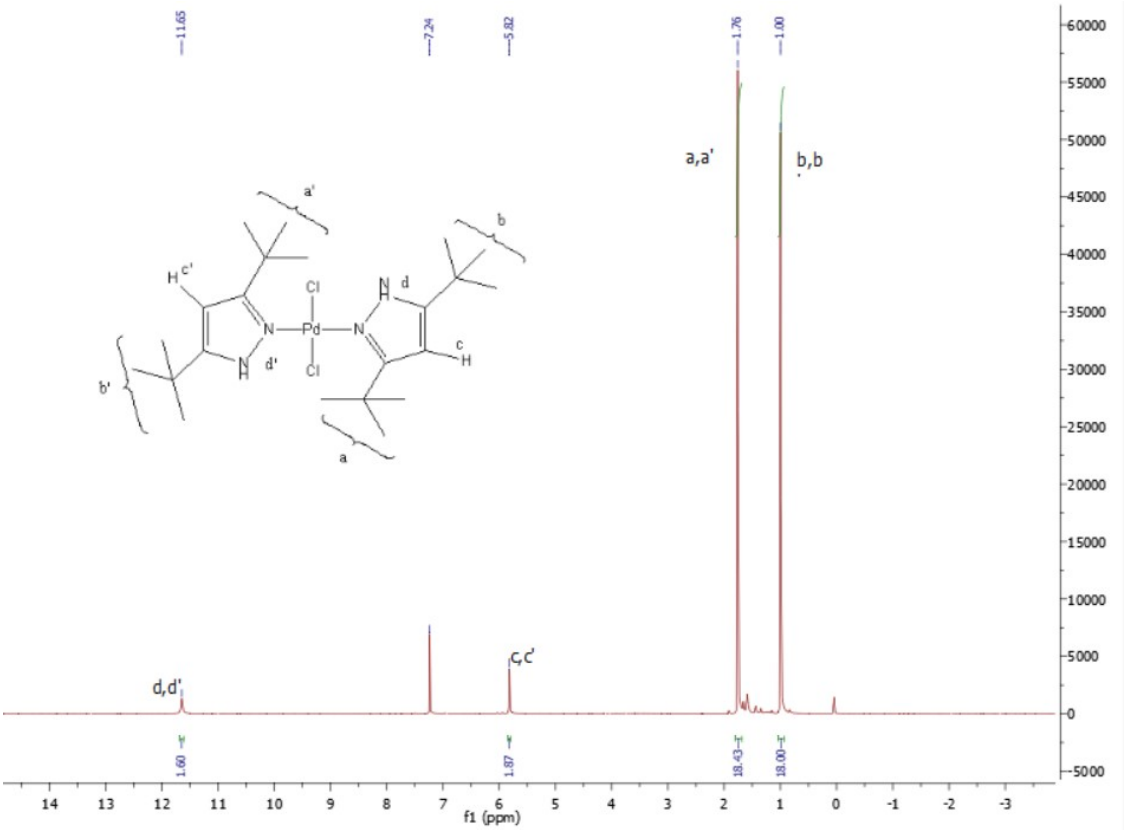


**Fig. S40** $^{1}H$ NMR spectrum of **5** recorded in $CDCl_3$.

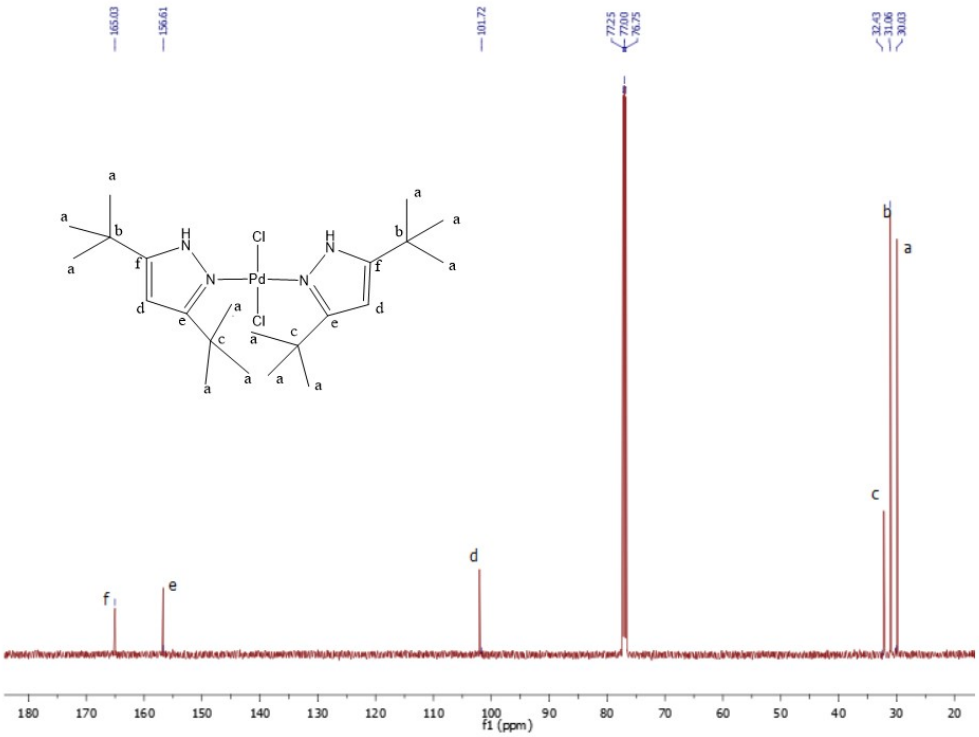

**Fig. S41** $^{13}C\{^{1}H\}$ NMR spectrum of **5** recorded in $CDCl_3$.

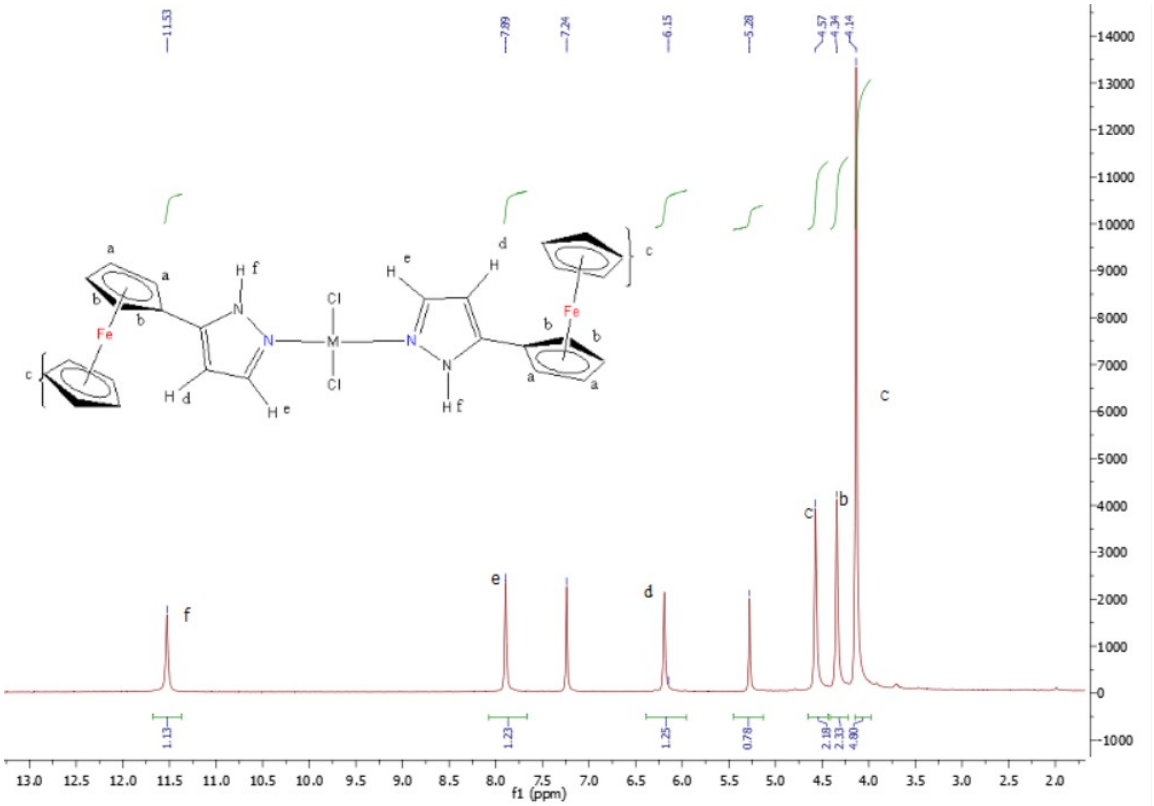

**Fig. S42** $^{1}H$ NMR spectrum of **6** recorded in $CDCl_3$.

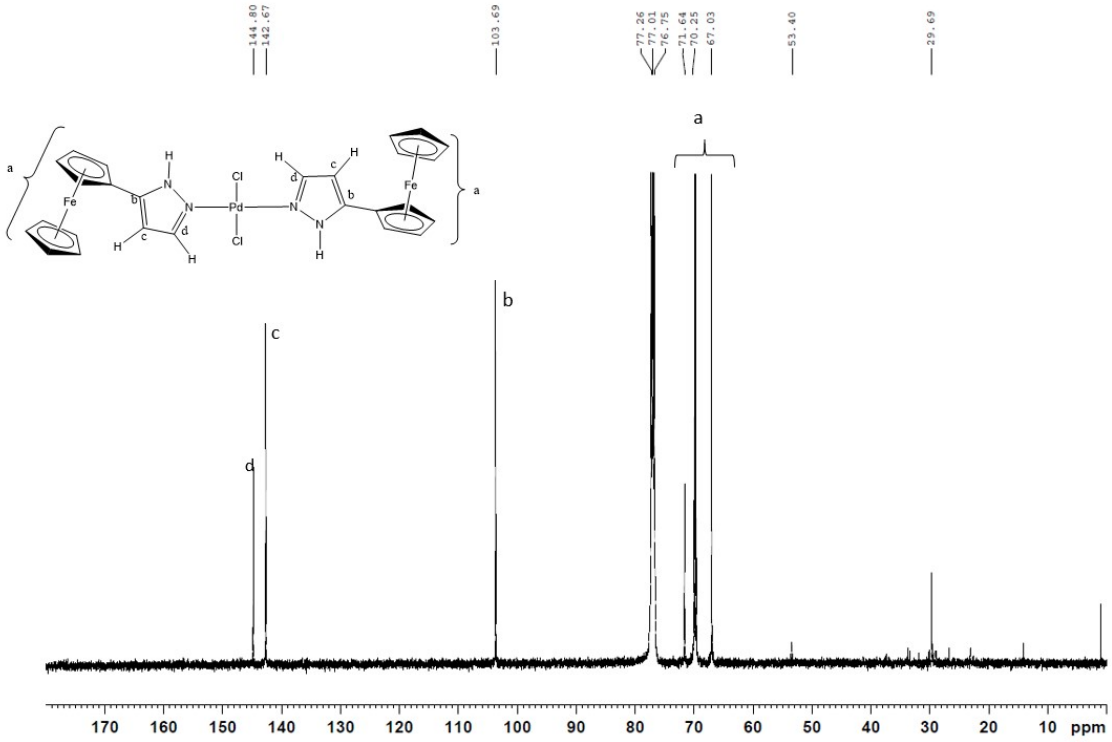


**Fig. S43** $^{13}C\{^{1}H\}$ NMR spectrum of **6** recorded in $CDCl_3$.

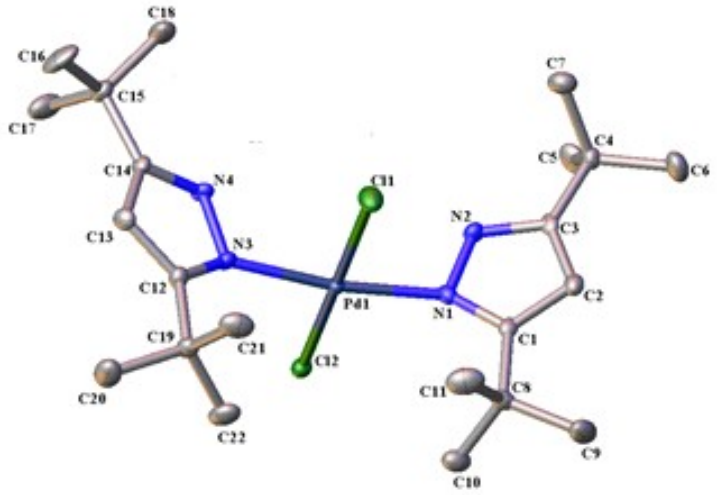


**Fig. S44** Molecular structure for complex **5**. Hydrogen atoms and distorted *ᵗBu* group omitted for clarity. Selected bond lengths (Å): Pd(1)–N(1), 2.012(2); Pd(1)–N(3), 2.018(2); Pd(1)–Cl(1), 2.2861(8); Pd(1)–Cl(2), 2.3332(8). Selected bond angles (°): Cl(1)–Pd(1)–Cl(2), 175.94 (3); N(1)–Pd(1)–Cl(1), 86.70(7); N(1)–Pd(1)–Cl(2), 92.14(7); N(1)–Pd–N(3), 171.86(9); N(3)–Pd(1)–Cl(1), 87.22(7); N(3)–Pd(1)–Cl(2), 93.56(7).

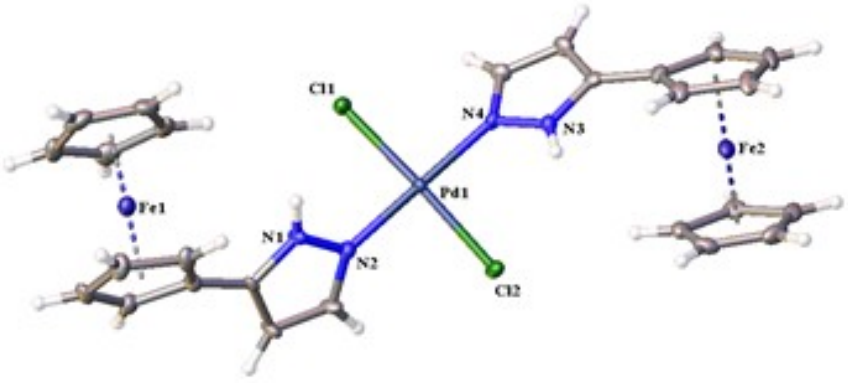


**Fig. S45** Molecular structure for complex **6**. Selected bond lengths (Å): Pd(1)–N(2), 1.999(4); Pd(1)–N(4), 2.007(4); Pd(1)–Cl(1), 2.3006(13); Pd(1)–Cl(2), 2.2063(12). Selected bond angles (°): Cl(1)–Pd(1)–Cl(2), 175.06(5); N(2)–Pd(1)–N(4), 179.72(18); N(2)–Pd(1)–Cl(1), 89.41(12); N(2)–Pd–Cl(2), 89.10(12); N(4)–Pd(1)–Cl(1), 90.81(12); N(4)–Pd(1)–Cl(2), 90.70(12).

**Table S2** Crystallographic data for complexes **5** and **6**

| | **5.$CHCl_3$** | **6.$CH_2Cl_2$** |
|---|---|---|
| Empirical formula | $C_{23}H_{41}Cl_5N_4Pd$ | $C_{27}H_{25.75}Cl_4Fe_2N_4Pd$ |
| Formula weight | 657.25 | 766.16 |
| Temperature/K | 99.96 | 100.02 |
| Crystal system | Monoclinic | triclinic |
| Space group | C2/c | P-1 |
| a/Å | 25.066(3) | 13.5082(16) |
| b/Å | 12.2089(11) | 18.204(2) |
| c/Å | 21.0499(18) | 24.120(3) |
| α/° | 90 | 107.316(2) |
| β/° | 106.859(4) | 90.970(3) |
| γ/° | 90 | 95.614(3) |
| Volume/$Å^3$ | 6164.9(10) | 5628.5(11) |
| Z | 8 | 8 |
| $\rho_{calc}g/cm^3$ | 1.416 | 1.808 |
| $\mu/mm^{-1}$ | 1.054 | 2.055 |
| F (000) | 2704.0 | 3054.0 |
| Radiation | MoKα (λ = 0.71073) | MoKα (λ = 0.71073) |
| 2Θ range for data collection/° | 3.744 to 49.964 | 1.77 to 50.882 |
| Reflections collected | 45923 | 93054 |
| Independent reflections | 5407 [$R_{int}$ = 0.1098, $R_{sigma}$ = 0.0691] | 20743 [$R_{int}$ = 0.0914, $R_{sigma}$ = 0.0926] |
| Data/restraints/ parameters | 5407/0/318 | 20743/0/1369 |
| Goodness-of-fit on $F^2$ | 1.045 | 1.060 |
| Final R indexes [I ≥ 2σ (I)] | $R_1$ = 0.0409, $wR_2$ = 0.1011 | $R_1$ = 0.0574, $wR_2$ = 0.1477 |
| Final R indexes [all data] | $R_1$ = 0.0474, $wR_2$ = 0.1053 | $R_1$ = 0.0713, $wR_2$ = 0.1601 |